



Published in final edited form as:

Nature. 2020 October ; 586(7829): 407–411. doi:10.1038/s41586-020-2793-8.

Amygdala inhibitory neurons as loci for translation in emotional memories

Prerana Shrestha^{1,‡}, Zhe Shan¹, Maggie Mamcarz¹, Karen San Agustin Ruiz¹, Adam T. Zerihoun¹, Chien-Yu Juan¹, Pedro M. Herrero-Vidal¹, Jerry Pelletier², Nathaniel Heintz³, Eric Klann^{1,4,‡}

¹Center for Neural Science, New York University, New York, NY 10003

²Department of Biochemistry, McGill University, Montreal, Quebec

³Laboratory of Molecular Biology, The Rockefeller University, New York, NY 10065

⁴NYU Neuroscience Institute, New York University School of Medicine, New York, NY

Abstract

To survive in a dynamic environment, animals need to identify and appropriately respond to stimuli that signal danger¹. Survival also depends on suppressing the threat-response during a stimulus that predicts absence of threat, i.e. safety^{2–5}. Understanding the biological substrates of emotional memories in which animals learn to flexibly execute defensive responses to a threat-predictive cue and a safety cue is critical for developing treatments for memory disorders such as PTSD⁵. A key brain area for processing and storing threat memories is the centrolateral amygdala (CeL), which is an important node in the neuronal circuit mediating defensive responses^{6–9}. Here, we applied intersectional chemogenetic strategies in CeL inhibitory neurons (INs) to block cell-type-specific translation programs that are sensitive to depletion of eukaryotic initiation factor 4E (eIF4E) and phosphorylation of eukaryotic initiation factor 2 α (p-eIF2 α), respectively. We show that de novo translation in CeL Somatostatin-expressing (SOM) INs is necessary for long-term storage of conditioned-threat response whereas de novo translation in CeL protein kinase C δ (PKC δ)-expressing INs is necessary for conditioned-response inhibition to a safety cue. Our results provide new insight into the role of de novo protein synthesis in distinct CeL inhibitory neuron populations during consolidation of long-term memories.

Neurons have evolved to both respond dynamically to their environment at millisecond time scales and yet can store information stably for a much longer period of time. The latter mode

Users may view, print, copy, and download text and data-mine the content in such documents, for the purposes of academic research, subject always to the full Conditions of use:http://www.nature.com/authors/editorial_policies/license.html#terms

[‡]Correspondence: eklann@cns.nyu.edu, ps755@nyu.edu.

AUTHOR CONTRIBUTIONS

P.S. and E.K. conceptualized the framework of this study. P.S. carried out surgeries, behavioral testing, and collected and analyzed data. Z.S. carried out western blots and behavior testing. M.M. performed mouse breeding and pharmacological treatments. K.S.A.R., A.T.Z., C.-Y.J. and P.M.H.-V. carried out mouse behavioral testing. J.P. generated and provided the floxed Col1a1 TRE GFP.shmiR-4E mice. N.H. generated and provided the floxed iPKR mice. P.S. and E.K. wrote the paper. All authors read and commented on the paper.

COMPETING FINANCIAL INTERESTS

The authors declare no competing financial interests.

of stabilizing information in mnemonic processes requires *de novo* translation^{10,11}. Tight regulation of translation occurs during initiation where the two major rate-limiting steps are the assembly of the eIF2-tRNA_i^{Met} ternary complex and the m⁷GpppN cap-binding complex¹². Bidirectional control of protein synthesis can be mediated by altering the levels of these two complexes. As part of the integrated stress response, eIF2 α kinases phosphorylate eIF2 α and this in turn inhibits the eIF2 guanine exchange factor eIF2B, effectively blocking recycling of the ternary complex to shutdown general translation. On the other hand, dephosphorylation of eIF2 α occurs following memory formation, allowing the requisite *de novo* translation to initiate¹³. Likewise, the formation of the m⁷GpppN cap-binding complex is essential for cap-dependent translation initiation. Central to the regulation of cap-dependent translation is the mammalian target of rapamycin complex I (mTORC1) signaling pathway. Activation of mTORC1 triggers initiation of cap-dependent translation via phosphorylation of eukaryotic initiation factor 4E (eIF4E)-binding proteins (4E-BPs) and p70 S6 kinase 1 (S6K1). Phosphorylation of 4E-BPs results in the release of eIF4E, which then becomes incorporated into the eIF4F complex, along with the modular scaffolding protein eIF4G and the RNA helicase eIF4A to initiate cap-dependent translation. Phosphorylation of S6K1 leads to phosphorylation of downstream targets including ribosomal protein S6, eIF4B, and PDCD4 that promote translation^{12, 14}. Although both eIF2 and mTORC1 pathways regulate key steps in translation initiation, these are generally viewed as separate translation control pathways with largely non-overlapping molecular outcomes^{15,16}.

We developed a differential threat-conditioning paradigm using interleaved presentations of a shock-predictive tone (paired conditioned-stimulus, CS+) that co-terminated with a footshock (unconditioned stimulus, US) and a safety-predictive tone that predicted absence of the footshock (CS-) within session (Fig. 1a). The Box-Only control group was placed in the training context but did not get exposed to either CS+ or CS- whereas the Unpaired training group was exposed to all three stimuli (CS+, CS- and US) in scrambled order, precluding any tone-shock contingency (Extended Data Fig. 1a). Compared to the Unpaired group, mice in the Paired training group learned the CS+-US association during training with escalating freezing response to successive CS presentations (Extended Data Fig. 1b–d) even though both groups increased freezing behavior post-tone (Extended Data Fig. 1e). When the mice were tested for long-term memory (LTM), paired training resulted in mice exhibiting a high freezing response to the CS+ while suppressing the response to CS- (Fig. 1b–c), with a robust discrimination-index outcome compared to Box-Only and Unpaired controls (Fig. 1d, Extended Data Fig. 1f). Notably, the freezing response to CS- was higher than the negligible freezing behavior during pre-CS period (Extended Data Fig. 1g, h). Increasing the number of CS+-US pairings from 3 to 5 increased freezing with successive CS presentations during memory acquisition (Extended Data Fig. 1i, j), but did not improve the freezing response to either the CS+ and CS- or the discrimination-index during LTM (Extended Data Fig. 1k, l), indicating that the learned behavior had reached an asymptote after 3 pairings. Biochemical analysis of the amygdala showed that activation of mTORC1, as indicated by phosphorylation of S6K1, occurs in Paired animals but not in Box-Only or Unpaired groups (Fig. 1e, f). Notably, dephosphorylation of eIF2 α occurred in the differentially threat-conditioned group as well as the Unpaired group, indicating pathway

divergence of translation programs in capturing the shock experience versus tone-shock contingencies (Fig. 1e, g). We next focused on SOM and PKC δ inhibitory neuron (IN) subpopulations^{17–19} that each constitute approximately half of all neurons in the CeL (Extended Data Fig. 2a–b) and are largely distinct (Fig. 1h, Extended Data Fig. 2c–e). We found that phosphorylation of ribosomal protein S6 at Ser 235/6 was significantly increased in both SOM and PKC δ INs in the Paired group compared to Box-Only and Unpaired controls, indicating activation of the mTORC1 pathway by differential threat-conditioning (Extended Data Fig. 2f–g). We then utilized *in vivo* surface sensing of translation (SUnSET) to label newly synthesized proteins with the synthetic tyrosyl-tRNA analog puromycin in awake behaving mice. A significant increase in *de novo* translation in CeL, specifically in PKC δ INs, was observed in the Paired group compared to both Unpaired and Box-only controls (Fig. 1h, Extended Data Fig. 3a–b).

To establish a causal role for cap-dependent translation in CeL INs in differential threat memories, we devised an intersectional chemogenetic strategy to stably knockdown eIF4E in SOM and PKC δ INs for a defined period. We used a knock-in mouse-based conditional expression of a synthetic micro-RNA specifically targeting *Eif4e* mRNA²⁰, consisting of *Eif4e*-specific shRNA embedded in the microRNA-30 backbone (shmiR) (Fig. 2a). shmiRs are driven by Pol II promoters and act as natural substrates in miRNA biogenesis pathways, leading to robust expression of mature shRNA and high knockdown efficiency²¹. The shmiR for *Eif4e* (shmiR-4E) is integrated in the 3' UTR of GFP and is under transcriptional regulation of tet-responsive elements (TRE). In double transgenic SOM-Cre::TRE-GFP.shmiR-4E and PKC δ -Cre::TRE-GFP.shmiR-4E mice, we virally expressed the Cre-dependent tet transactivator (tTA) in the CeL while placing the animals on Off-Dox diet for 14 days following viral delivery to mediate eIF4E knockdown (4Ekd) (Fig. 2b, Extended Data Fig. 4a–b). This strategy resulted in significant reduction of eIF4E protein (Extended Data Fig. 4c–d) and subsequently, in a significant inhibition of *de novo* global translation in CeL INs compared to GFP controls (Extended Data Fig. 4e–f). MMP9, the protein product of an eIF4E-sensitive mRNA important for long-lasting synaptic plasticity in the central amygdala²² was also significantly reduced in SOM and PKC δ INs (Extended Data Fig. 4g–h). At the level of behavior, eIF4E knockdown in SOM INs did not affect spontaneous locomotion in the open field and elevated plus maze (Extended Data Fig. 5a–h). However, PKC δ .4Ekd mice, despite exhibiting normal open field activity (Extended Fig. 5i–m), explored the open arm of elevated plus maze significantly more than the control animals indicating reduced anxiety (Extended Data Fig. 5n–p). Anxiolysis with cap-dependent translation inhibition in PKC δ INs is consistent with a previous report that optogenetically silencing PKC δ neurons in CeL decreases anxiety²³.

To test whether inhibition of cap-dependent translation in CeL interneuron subtypes has any impact on long-term threat memories, we trained SOM and PKC δ animals in simple cued threat-conditioning paradigm where a tone unambiguously co-terminated with a footshock (Fig. 2c, Extended Data Fig. 6a). Although all mice learned the CS-US association equivalently (Fig. 2d, Extended Data Fig. 6b), only SOM.4Ekd mice displayed a significant LTM deficit (Fig. 2e, Extended Data Fig. 6c). SOM.4Ekd mice that were placed on Dox diet for 14 days allowing eIF4E re-expression and then re-trained in the same protocol displayed complete rescue of LTM (Fig. 2f). Next, we tested 4Ekd animals in the differential threat-

conditioning paradigm (Fig. 1a). SOM.4Ekd mice learned equivalently to SOM.GFP mice (Extended Data Fig. 6d–f). During LTM, SOM.4Ekd mice displayed a selective impairment in the conditioned-threat response to CS+ and yet exhibited a normal safety response to CS- and a normal cue discrimination-index (Fig. 2g–i). PKC δ .4Ekd mice also acquired differential threat associative memory normally (Extended Data Fig. 6g–i). However, PKC δ .4Ekd mice displayed a selective impairment in the conditioned-safety response to CS- despite exhibiting a normal conditioned-threat response to CS+ (Fig. 2g, j), which led to a sub-optimal cue discrimination-index for PKC δ .4Ekd animals (Fig. 2k). Both SOM and PKC δ .4Ekd animals displayed negligible baseline freezing during pre-CS (Extended Data Fig. 6j–m). Overall, these results show that blocking cap-dependent translation in SOM and PKC δ INs results in selective impairment in conditioned threat and safety responses, respectively.

To understand the contribution of time-limited *de novo* protein synthesis during the initial consolidation window following learning, we applied a knock-in mouse-based chemogenetic strategy that we recently developed¹⁰ to express Cre-dependent and drug-inducible double-stranded RNA activated protein kinase (iPKR) in SOM and PKC δ INs (Fig. 3a). Because the iPKR mouse line also enables Cre-dependent expression of EGFP-tagged ribosomal subunit L10, we detected soma-localized GFP in the CeL SOM and PKC δ neurons of SOM.iPKR and PKC δ .iPKR mice, respectively (Fig. 3b). *In vivo* infusion of ASV, the drug inducer of iPKR, significantly elevated phosphorylation of eIF2 α (S51) in SOM and PKC δ INs in the CeL (Extended Data Fig. 7a–b). We then exposed the animals to the differential threat-conditioning paradigm as described above, but restricted cell type-specific protein synthesis inhibition (ciPSI) to the initial consolidation period with intra-CeL infusion of ASV immediately after training (Fig. 3c). Although all mice learned equivalently during training (Extended Data Fig. 7c–h), we found that the memory deficits were remarkably divergent in the SOM.iPKR and PKC δ .iPKR mice. Similar to the 4Ekd approach, we found that blocking general translation with increased eIF2 α phosphorylation in SOM INs impaired the freezing response to CS+ while keeping the safety response and cue discrimination intact (Fig. 3d–f). On the other hand, blocking general translation with increased eIF2 α phosphorylation in PKC δ INs resulted in an impaired safety response and cue discrimination, with no reduction in freezing response to CS+ during LTM (Fig. 3d, g, h). These findings demonstrate that the simultaneous consolidation of long-lasting threat and safety responses requires *de novo* protein synthesis in distinct populations of inhibitory neurons in centrolateral amygdala.

Protein synthesis machinery within neurons is modulated by events at the cell membrane that communicate trans-synaptic inputs via intracellular signaling cascades. We thus examined the conserved cell-autonomous G α_i and G α_q protein signaling pathways in CeL INs using viral expression of designer receptors activated by designer drugs (DREADDs) that are based on mutant muscarinic acetylcholine receptors and couple to G proteins²⁴ (Fig. 4a, b). Specifically, G α_i signaling leads to inhibition of adenylyl cyclase and decreases neuronal activity, whereas G α_q protein signaling results in activation of phospholipase C and can boost *de novo* translation^{10, 24}. In differential threat-conditioning paradigm, pre-training administration of DREADD agonist C21 did not alter learning in SOM.tdT, SOM.hM4Di or SOM.hM3Dq animals (Extended Data Fig. 8a–i). During memory retrieval, C21 exerted opposite behavioral effects on SOM.hM4Di and SOM.hM3Dq animals, while the drug had

no effect in control SOM.tdT animals (Extended Data Fig. 8j, k). C21 treatment significantly decreased the conditioned-threat response to CS+ in SOM.hM4Di mice (Fig. 4c). This threat-response deficit caused by activating $G_{\alpha i}$ protein signaling in SOM INs is consistent with behavioral effects of *de novo* translation inhibition in these CeL INs. In contrast, increasing neuronal activity in SOM INs by activating $G_{\alpha q}$ pathway during threat-conditioning resulted in enhanced CS+ LTM (Fig. 4d) supporting bidirectional modulation of the threat-response with chemogenetic manipulation of conserved G-protein signaling in SOM INs, consistent with previous findings^{1,3}. C21 did not alter cued threat discrimination index (Fig. 4e) or baseline freezing during pre-CS of both memory acquisition and retrieval phases (Extended Data Fig. 8l, m). Likewise, DREADD manipulation of PKC δ INs did not alter associative learning in PKC δ .tdT, PKC δ .hM4Di or PKC δ .hM3Dq animals (Extended Data Fig. 9a–i). Notably, activation of $G_{\alpha i}$ protein signaling pathway in PKC δ INs in PKC δ .hM4Di +C21 mice led to a selective impairment in safety response to CS- and cue discrimination (Fig. 4f, h) whereas activating the $G_{\alpha q}$ pathway in PKC δ INs reduced the threat-response to CS+ (Fig. 4g, h). C21 had no effect on memory retrieval in PKC δ .tdT mice (Extended Data Fig. 9j, k) as well as on baseline freezing during pre-CS of both memory acquisition and retrieval phases (Extended Data Fig. 9l, m). These data indicate that $G_{\alpha i}$ protein signaling mirrors the effect of blocking *de novo* protein synthesis in PKC δ INs. On the other hand, activating $G_{\alpha q}$ pathway in CeL SOM and PKC δ INs have opposite effects on CS+ threat-response but do not alter CS- safety response.

Previous studies have reported enhancement of long-term spatial and threat memories by relieving translation repression with constitutive deletion of genes encoding eIF2 α kinases such as GCN2 and PKR^{36,37} or by administering ISRIB, an eIF2B activator²⁵. Likewise, constitutive deletion of the gene encoding the eIF4E repressor 4E-BP2 results in enhanced conditioned taste aversion memory²⁶ whereas acute intra-amygdalar infusion of 4EGI-1, an inhibitor of eIF4E-eIF4G interaction, blocks threat memory consolidation²⁷. In both simple and differential threat-conditioning paradigms, our results show that eIF2- as well as eIF4E-dependent translation programs in CeL SOM INs are required for the conditioned-threat response, which indicates that SOM INs are the primary CeL locus for storage of cued threat memory. Our findings are consistent with studies showing long-lasting synaptic potentiation in CeL SOM inhibitory neurons following threat learning that lasts at least 24 hours¹⁷. Moreover, expressing biallelic phosphomutant eIF2 α in SOM INs brainwide results in enhanced cued and contextual LTM²⁸. In a contrasting but complementary role, *de novo* translation in PKC δ INs serves to store the conditioned-safety response. Our findings thus support a working model where CeL SOM and PKC δ INs simultaneously store threat and safety cue-associated memories by changing the cellular translation landscape (Extended Data Fig. 10).

Threat generalization due to impaired safety response is a hallmark feature of PTSD⁵. In auditory threat conditioning, overtraining or increasing US intensity has been shown to increase auditory threat generalization²⁹. Cells in the lateral amygdala shift the threat-response from cue-specific to cue generalization depending on the US intensity³⁰. Within the centrolateral amygdala, PKC δ INs are direct recipients of US-related nociceptive input from the parabrachial nucleus⁸. Our current findings that blocking neuronal activity and *de novo* protein synthesis in CeL PKC δ INs disrupts the acquisition and consolidation of long-

term conditioned-response inhibition to the non-reinforced tone (CS-) is in agreement with the US-processing feature of these types of neurons. To conclude, our study provides the first evidence that disruption of protein synthesis in discrete interneuron subpopulations in the centrolateral amygdala impairs associative memories related to threat and safety, which may contribute to maladaptive behavior in memory disorders such as PTSD.

METHODS

Animals

Mice were provided with food and water ad libitum and were maintained in a 12h/12h light/dark cycle at New York University at stable temperature (78°F) and humidity (40 to 50%). All mice were backcrossed to C57Bl/6J strain for at least 5 generations. Both male and female mice, aged 3–6 months, were used in all experiments. Somatostatin IRES-Cre knockin mice (SOM-Cre; stock #013044) were obtained from Jackson labs. PKC δ ::GluCl α -iCre BAC transgenic mice (PKC δ -Cre)⁹ were generated by GENSAT and kindly provided by Dr. David Anderson (Caltech). Cre reporter lines including Floxed TRAP (stock #022367) mice expressing GFP-L10 fusion protein in a Cre-dependent manner, and Floxed tdTomato mice (Ai14; stock #007908) that express tdTomato in a Cre-dependent manner were obtained from Jackson labs. Coll1a1^{TRE GFP.shmiR-4E.389} mice were generated as previously described²⁶. Floxed iPKR (Eef1a1^{LSL.NS3/4.TRAP.iPKR}) mice were generated as previously described¹⁰. SOM-Cre and PKC δ -Cre mice were crossed with floxed Coll1a1^{TRE GFP.shmiR-4E} mice to generate transheterozygote SOM-Cre::TRE-GFP.shmiR-4E and PKC δ -Cre::TRE-GFP.shmiR-4E mice respectively. Likewise, SOM-Cre and PKC δ -Cre mice were crossed with floxed iPKR mice to generate transheterozygote SOM.iPKR and PKC δ .iPKR mice respectively. SOM.tdT and PKC δ .tdT mice were generated by crossing SOM-Cre and PKC δ -Cre with floxed tdTomato reporter line, whereas PKC δ .TRAP mice were generated by crossing PKC δ -Cre line with floxed TRAP mice. SOM.tdT.TRE-GFP.shmiR-eIF4E and PKC δ .tdT.TRE-GFP.shmiR-eIF4E mice were generated by breeding SOM-Cre::TRE-GFP.shmiR-4E and PKC δ -Cre::TRE-GFP.shmiR-4E mice with homozygous floxed tdTomato reporter line. Wildtype C57Bl/6J mice (stock #000664) were purchased from Jackson labs.

Drugs and chemicals

Doxycycline was added to rodent chow at 40 mg/kg (Bio-Serv, F4159). This doxycycline diet was provided to SOM.4Ekd, PKC δ .4Ekd, and control SOM.WT and PKC δ .WT mice starting from the day of surgery for 7d and to SOM.4Ekd re-training group for 14d after LTM1 *ad libitum*. Asunaprevir (ASV, ChemExpress) was dissolved in DMSO to a stock concentration of 10 mM and diluted in sterile saline to 100 nM. 0.5 μ l of this drug was intracranially infused into the centrolateral amygdala (-1.22 mm anteroposterior AP, +/- -3.00 mm ML, -4.60 mm DV) of SOM.iPKR and PKC δ .iPKR animals using an injection cannula inserted into the stainless-steel guide cannula (Plastics One). ASV infusion was carried out at 0.125 μ l/min using an injection cannula extending out of PE50 tubing attached to a 5 μ l Hamilton syringe (Hamilton) using a PHD 2000 Infusion Pump (Harvard Apparatus). After injection, the injection cannula was kept in place for 1 min before its withdrawal. Puromycin (Sigma, P8833) was dissolved in ddH₂O at 25 μ g/ μ l, and this stock

was freshly diluted in saline to 10 $\mu\text{g}/\mu\text{l}$ for SUNSET assays *in vivo*. Digitonin (Sigma, D141) was dissolved in ddH₂O at 5% w/v to prepare the stock solution, which was diluted to 0.0015% w/v in 0.1 M PBS. Stock solution of aqueous 32% paraformaldehyde (EMS, 15714) was freshly diluted to 4% in 0.1 M PBS for transcardial perfusions and post-fixation of brain slices. The DREADD actuator, agonist C21 (Tocris 5548), was dissolved in DMSO at 40 mg ml⁻¹ concentration, freshly diluted in saline and administered to mice at 1 mg/kg intraperitoneally.

Stereotaxic surgeries

Mice were anesthetized with the mixture of ketamine (100 mg/kg) and xylazine (10 mg/kg) in sterile saline (i.p. injection). Stereotaxic surgeries were carried out on the Kopf stereotaxic instrument (Model 942), which was equipped with a microinjection unit (Model 5000). Viral vectors were injected intracranially using 2.0 μl Neuros syringe (Hamilton, #65459-02). Postoperative analgesia was delivered using subcutaneous injections of ketoprofen (3 mg/kg) for 3 days starting from the day of surgery. To generate SOM.4Ekd and PKC δ .4Ekd mice, 300 nl of AAV9.CAG Pr.DIO.tTA (1.0×10^{13} GC/ml; Vigene) was injected into the centrolateral amygdala (CeL) [-1.22 mm anterior posterior (AP), +/- 3.00 mm mediolateral (ML) and -4.60 mm dorsoventral (DV)] of double transheterozygote SOM-Cre::TRE-GFP.shmiR-4E and PKC δ -Cre::TRE-GFP.shmiR-4E mice. The plasmid encoding tet transactivator in a Cre-selective manner and under the transcriptional control of CAG promoter (pAAV.CAG Pr.DIO.tTA) was kindly provided by Hongkui Zeng (Allen Institute for Brain Science). For DREADD experiments, SOM-Cre and PKC δ -Cre mice were injected with 300 nl of AAV8.hSyn Pr.DIO.hM3Dq-mCherry (4×10^{12} vg/mL; Addgene #44361-AAV8) or AAV9.hSyn Pr.DIO.hM4Di-mCherry (1×10^{13} vg/mL, Addgene # 44362-AAV9). For controls, wild-type SOM and PKC δ mice were injected in CeL with 100 nl of AAV9.CAG Pr.DIO.GFP (3.33×10^{13} GC/ml, Penn Vector Core #CS1171) to generate SOM.GFP and PKC δ .GFP mice. Behavior and histology experiments for all viral vector injected animals were carried out 2–3 weeks after surgery. A cohort of SOM.iPKR and PKC δ .iPKR mice were injected with bilaterally in CeL with 200 nl of AAV.Eef1a1 Pr.DIO.EGFP-L10a (7×10^{12} GC/ml; Addgene #98747) for immunohistochemistry experiments. Intracranial cannula implant surgeries were carried out using custom-designed guide cannulas (Plastics One) along with a skull screw (1.6 mm shaft) to stabilize the dental cement, Metabond quick adhesive cement (Parkell S380), encapsulating the skull surface. For *in vivo* surface labeling of translation (SUNSET), SOM.4Ekd, PKC δ .4Ekd and control animals were implanted with a 23 gauge stainless steel guide cannula in right CeL (-1.22 mm AP, +3.00 mm ML and -2.40 mm DV) for puromycin infusion using an internal cannula with 2 mm projection. Similarly, SOM.iPKR and PKC δ .iPKR mice were also implanted with the 23-gauge stainless steel cannulas in CeL bilaterally for ASV infusions.

Behavior

All behavior sessions were conducted during the light cycle. Both male and female mice were included in all behavior experiments. Mice were randomly assigned for experimental conditions including drug or vehicle infusions, and for the order of testing in any given experimental paradigm. All behavior data were collected by experimenters blind to the genotype and experimental conditions. SOM.4Ekd, PKC δ .4Ekd and control mice were

trained in threat-conditioning paradigms after 14 days of eIF4E knockdown (Off Dox). A separate group of SOM.4Ekd, PKC δ .4Ekd and control mice were tested in the open field arena and elevated plus maze test after the same duration of eIF4E knockdown. SOM.iPKR and PKC δ .iPKR animals were trained in threat-conditioning paradigms 10 days after cannula implant surgeries to allow time for recovery.

Open field activity

Mice were placed in the center of an open field (27.31 \times 27.31 \times 20.32 cm) for 15 min during which a computer-operated optical system (Activity monitor software, Med Associates) monitored the spontaneous movement of the mice as they explored the arena. The parameters tested were distance traveled, and the ratio of center to total time.

Elevated plus maze

The plus maze consisted of two open arms (30 cm \times 5 cm) and two enclosed arms of the same size with 14-cm high sidewalls and an endwall. The arms extended from a common central square (5 cm² \times 5 cm²) perpendicular to each other, making the shape of a plus sign. The entire plus-maze apparatus was elevated to a height of 38.5 cm. Testing began by placing a mouse on the central platform of the maze facing the open arm. Standard 5-min test duration was applied, and the maze was wiped with 30% ethanol in between trials. Ethovision XT13 software (Noldus) was used to record the time spent on open arms and closed arms, total distance moved, and number of open arm and closed arm entries.

Simple cued threat-conditioning

Mice were habituated for 15 min in the threat-conditioning chambers housed inside sound attenuated cubicles (Coulbourn instruments) for 1 day. The habituation and training context included a metal grid floor and a white houselight. For simple threat-conditioning, mice were placed in the context for 270s and then presented twice with a 5kHz, 85 dB pure tone for 30s that co-terminated with a 2s 0.5mA footshock. The intertrial interval (ITI) was 2 min and after the second tone-shock presentation, mice remained in the chamber for an additional 120s. Cued threat-conditioning (cTC) LTM was tested 24h after training, in a novel context (Context B: vanilla scented cellulose bedding, plexiglas platform, and red houselight) with three presentations of paired tone (conditioned stimulus, CS). Freezing behavior was automatically measured by Freeze Frame software (ActiMetrics) and manually re-scored and verified by an experimenter blind to the genotype/drug. Motion traces were generated using the Freeze Frame software.

Differential cued threat-conditioning

For standard differential threat-conditioning, mice were placed in the training context for 250s and then trained with interleaved presentations of three paired tones or CS+ (7.5 kHz pulsatile tone, 50% duty cycle) that co-terminated with a 0.5 mA footshock and three unpaired tones or CS- (3 kHz pure tone) in the training context with variable ITI. Specifically, the CS+ (7.5 kHz) was presented at 270, 440 and 570 s and were paired with a footshock, whereas the 3 kHz pure tone occurred at 370, 520 and 660 s. The following day, cued threat discrimination (cTD) LTM was tested with 3 interleaved presentations of CS+

and CS- tones with the order reversed from the training day and with variable intertrial intervals. Specifically, the 3kHz CS- tone was presented at 250, 380 and 550s, whereas the 7.5kHz pulsed tone was presented at 310, 450 and 630 s. All tones lasted for 30 s. After the last CS- tone, mice remained in the testing context for an additional 60 s. When specifically stated, the CS- tones were assigned as 1 kHz pure tone. Box-Only control group were placed in the training context for the same duration as the cTD (Paired) group but they did not receive any footshock or were exposed to either CS+ or CS-. Unpaired control group were presented with three interleaved presentations of CS+ and CS- like the cTD (Paired) group, however the US was presented in between the CSs with no tone-shock contingency. All groups of mice (Box-Only, Paired and Unpaired) were tested the following day with three presentations of CS+ and CS- in reverse sequence compared to the training day. For Paired 5X group, animals were exposed to five presentations of CS+ (7.5 kHz pulsatile tone) that co-terminated with the footshock and five presentations of CS- (3 kHz pure tone) during training and tested with three interleaved presentations of CS+ and CS- during LTM 24h later.

Freezing behavior was automatically measured by Freeze Frame software (ActiMetrics) and manually re-scored and verified by an experimenter blind to the genotype/drug. Motion traces were generated using the Freeze Frame software. Discrimination-index was calculated as follows:

$$Discrimination\ Index = \frac{\frac{\sum_{i=1}^N CS+i}{N} - \frac{\sum_{i=1}^N CS-i}{N}}{\frac{\sum_{i=1}^N CS+i}{N} + \frac{\sum_{i=1}^N CS-i}{N}}$$

where,

N = number of animals

CS+ = freezing response to threat-predictive tone CS+ (%)

CS- = freezing response to safety-predictive tone CS- (%).

Western blot

Mice were euthanized by cervical dislocation. 300- μ m thick brain slices containing amygdala [Bregma -1.22 mm to -2.06 mm] were prepared in cold (4°C) carboxygenated (95% O₂, 5% CO₂) cutting solution (110 mM sucrose, 60 mM NaCl, 3 mM KCl, 1.25 mM NaH₂PO₄, 28 mM NaHCO₃, 5 mM Glucose, 0.6 mM Ascorbate, 7 mM MgCl₂ and 0.5 mM CaCl₂) using a VT1200S vibratome (Leica). The amygdala was micro-dissected from the brain slices and sonicated in ice-cold homogenization buffer (10 mM HEPES, 150 mM NaCl, 50 mM NaF, 1 mM EDTA, 1 mM EGTA, 10 mM Na₄P₂O₇, 1% Triton X-100, 0.1% SDS and 10% glycerol) that was freshly supplemented with 10 μ l each of protease inhibitor (Sigma) and phosphatase inhibitor (Sigma) per ml of homogenization buffer. Protein concentrations were measured using BCA assay (GE Healthcare). Samples were prepared with 5X sample buffer (0.25 M Tris-HCl pH6.8, 10% SDS, 0.05% bromophenol blue, 50%

glycerol and 25% - β mercaptoethanol) and heat denatured at 95°C for 5 min. 40 μ g protein per lane was run in pre-cast 4–12% Bis-Tris gels (Invitrogen) and subjected to SDS-PAGE followed by wet gel transfer to PVDF membranes. After blocking in 5% non-fat dry milk in 0.1M PBS with 0.1% Tween-20 (PBST), membranes were probed overnight at 4°C using primary antibodies (rabbit anti-p S6 (S235/236) 1:1000 (Cell Signaling #4858), rabbit anti-p-S6K1 Thr389 1:500 (Cell Signaling #9205), rabbit anti- S6K1 1:500 (Cell Signaling #2708), rabbit anti-p eIF2 α Ser51 1:300 (Cell Signaling #9721), rabbit eIF2 α 1:1000 (Cell Signaling #9722), mouse anti- β tubulin 1:5000 (Sigma #T8328) and mouse anti- β actin 1:5000 (Sigma #A5441). After washing 3 times in 0.1% PBST, membranes were probed with horseradish peroxidase-conjugated secondary IgG (1:5000) (Millipore #AP307P and #AP308P) for 1h at RT. Signals from membranes were detected with ECL chemiluminescence (Thermo Pierce) using Protein Simple instrument. Exposures were set to obtain signals at the linear range and then normalized by total protein and quantified via densitometry using ImageJ software.

***In vivo* surface labeling of translation (SUNSET)**

Awake behaving mice with intracranial cannula implants were infused with 5 μ g puromycin (0.5 μ l, 10 μ g/ μ l) in the central amygdala using PHD2000 infusion pump and Hamilton 5.0 μ l syringe. Mice were returned to the home cage and translation labeling with puromycin was carried out for 1h. Mice were deeply anesthetized with a mixture of ketamine (150 mg/kg) and xylazine (15 mg/kg), and transcardially perfused with 0.1M PBS, 0.0015% digitonin followed by 4% paraformaldehyde (PFA) in PBS. Brains were extracted and postfixed in 4% PFA for 24h, followed by immunohistochemistry.

Immunohistochemistry

Mice were deeply anesthetized with a mixture of ketamine (150 mg/kg) and xylazine (15 mg/kg), and transcardially perfused with 0.1M PBS followed by 4% paraformaldehyde in PBS. Brains were removed and postfixed in 4% PFA for 24h. 40 μ m free-floating coronal brain sections containing amygdala were collected using Leica vibratome (VT1000s) and stored in 1X PBS containing 0.05% Na-azide at 4°C. After blocking in 5% normal goat serum in 0.1M PBS with 0.1% Triton X-100, brain sections were probed overnight with primary antibodies (chicken anti-EGFP (abcam #ab13970 1:500; for PKC δ .TRAP, SOM.4Ekd and PKC δ 4Ekd brain sections), rabbit anti-EGFP 1:300 (Thermo Fisher #G10362; for SOM.iPKR and PKC δ .iPKR brain sections), rabbit anti-pS6 (S235/6) 1:1000 (Cell Signaling #4858), rabbit anti-p-eIF2 α S51 1:300 (Cell Signaling #9721), rabbit anti-eIF4E 1:500 (Bethyl #A301–153A), rabbit anti-Mmp9 1:300 (abcam #ab38898), mouse NeuN 1:2000 (Millipore Sigma #MAB377), chicken anti-Somatostatin 1:300 (Synaptic Systems #366 006), rabbit anti- PKC δ 1:250 (abcam #ab182126), guinea pig anti-RFP 1:500 (Synaptic systems #390 004), and mouse anti-puromycin 1:1000 (Millipore Sigma #MABE343). After washing three times in 0.1 M PBS, brain sections were incubated with Alexa Fluor conjugated secondary antibodies 1:200 (Abcam #ab175674, #ab175651; Thermo Fisher #A-111034, #A11012, #A21245, #A11073, #A121236, #A21206) in blocking buffer for 1.5h at RT, and mounted using Prolong Gold antifade mountant with DAPI or without DAPI (Life Technologies #P36931, #P36930).

Single molecule fluorescence in situ hybridization

Mouse brains were collected through flash freezing in OCT Tissue Tek medium (VWR #25608–930) in dry ice. Using a cryostat, each brain was serially sectioned at 20 μm and thaw-mounted onto Superfrost plus slides spanning AP -1.22 mm to AP -1.70 mm. Slides were stored at -80°C . Single molecule fluorescent in situ hybridization (smFISH) was performed using a RNAscope fluorescent multiplex kit (ACD Bio #320850). *Sst* (#404631-C2), and *Prkcd* (#44191-C3) probes were purchased from the Advanced Cell Diagnostics catalog. Brain sections were fixed in 4% paraformaldehyde for 15 min and then washed in 50%, 70%, 100% and 100% ethanol for 5 min each. Slides were dried for 10 min and hydrophobic barrier drawn around the sections using ImmEdge hydrophobic barrier pen (ACD Bio #310018). Proteins were digested using protease solution (Protease IV) for 30 min at RT. Immediately afterward, slides were washed twice in 0.1 M PBS. C2 and C3 probes were heated in 40°C water bath for 10 min, and brought to RT for additional 10 min. Probes were applied to the slides in a humidified incubator (ACD Bio #321711) for 2h. Slides were rinsed twice in RNAscope wash buffer and then underwent the colorimetric reaction steps according to manufacturer's instructions using AMP4-Alt C (C2, far red; C3, green). After the final wash buffer, slides were immediately coverslipped using Prolong Gold Antifade mounting medium with DAPI.

Image analysis

Imaging data for the whole coronal brain section were acquired using Olympus slide scanner (VS120) for qualitative visualization of transgene expression and viral gene targeting, and analyzed in ImageJ using the BIOP VSI reader plugin. Imaging data from immunohistochemistry and smFISH experiments were acquired using an SP8 confocal microscope (Leica) with 20X objective lens (with 1X or 2X zoom) and z-stacks (approximately 6 optical sections with 0.563 μm step size) for three coronal sections per mouse from AP -1.22 mm to -1.70 mm ($n=3$ mice) were collected. Imaging data was analyzed with ImageJ using the Bio-Formats importer plugin. Maximum projection of the z-stacks was generated followed by manual outline of individual cells and mean fluorescence intensity measurements using the drawing and measure tools. Mean fluorescence intensity values for all cell measurements were normalized to the mean fluorescence intensity for controls.

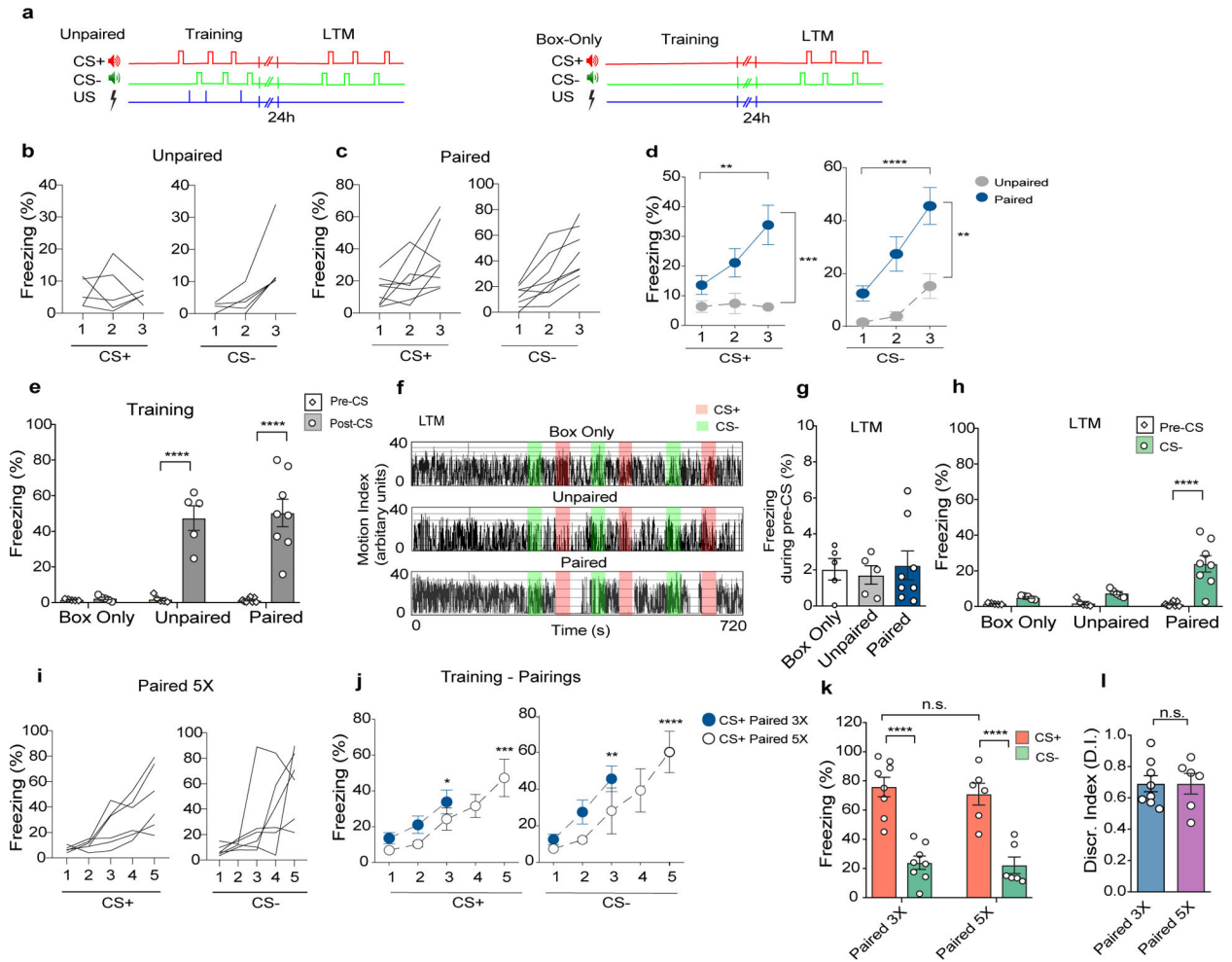
Statistics

Statistical analyses were performed using GraphPad Prism 8 (GraphPad software) for all datasets. Data are expressed as mean \pm SEM. Data from two groups were compared using two-tailed unpaired Student's t test. Multiple group comparisons were conducted using one-way ANOVA, or two-way ANOVA, with post hoc tests as described in the appropriate figure legend. Statistical analysis was performed with an α level of 0.05. p values <0.05 were considered significant.

DATA AVAILABILITY

Details of the statistical analyses are provided in a supplementary document. Raw behavior data that are used in this study are available from the corresponding authors upon request.

Extended Data



Extended Data Figure 1. Differential cued threat conditioning.

- a) Schematic of the behavior protocol for the Unpaired group (left) and Box-Only control group (right).
- b) Freezing response to CS+ and CS- in individual animals trained using the Unpaired behavior protocol.
- c) Freezing response to CS+ and CS- in individual animals trained using the Paired behavior protocol.
- d) Paired group learned the association between CS+ and US and showed increasing freezing response to successive CS presentations whereas the Unpaired group did not associate CS+ with US. RM Two-way ANOVA with Bonferroni's post-hoc test. Effect of CS + training: $F(1,11)=11.40$, $p=0.0062$; effect of CS- training: $F(2,33)=9.360$, $p=0.0006$. $n[\text{Unpaired}]=5$ and $n[\text{Paired}]=8$ animals.
- e) Both Paired and Unpaired groups, but not Box-Only group, increased freezing levels during the post-tone period compared to the pre-tone period. Two way ANOVA with Bonferroni's post hoc test. Effect of training: $F(2,30)=13.86$, $p<0.0001$, effect of epoch: $F(1,30)=60.38$, $p<0.0001$. $n[\text{Box-Only}]=5$, $n[\text{Unpaired}]=5$ and $n[\text{Paired}]=8$ animals.

f) Representative motion traces for Box-Only, Unpaired and Paired groups during LTM.

g) Freezing response during pre-CS of LTM test is low for all three groups. One-way ANOVA. $p=0.874$. $n[\text{Box-Only}]=5$, $n[\text{Unpaired}]=5$ and $n[\text{Paired}]=8$ animals.

h) Animals in the Paired group freeze significantly higher during CS- than during the pre-tone period. Two-way ANOVA with Bonferroni's post-hoc test. Effect of training: $F(2,30)=8.38$, $p=0.0013$; effect of epoch: $F(1,30)=23.97$, $p<0.0001$. $n[\text{Box-Only}]=5$, $n[\text{Unpaired}]=5$ and $n[\text{Paired}]=8$ animals.

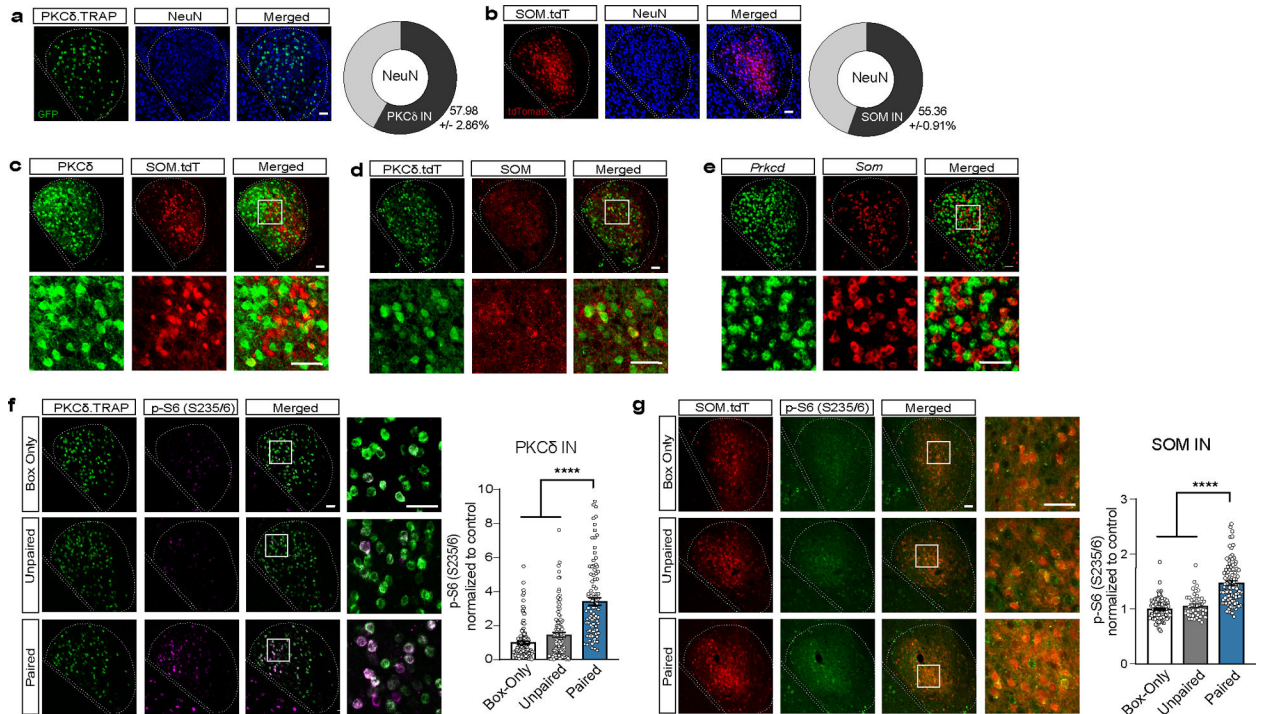
i) Freezing response to CS+ and CS- in individual animals trained using the Paired 5X behavior protocol.

j) Increasing the number of CS-US pairs from 3 to 5 pairings during training led to a continued escalation of freezing response to successive presentations of CS's. RM Two-way ANOVA with Bonferroni's post-hoc test. Effect of CS+: $F(1,24)=23.95$, $p<0.0001$; effect of CS-: $F(1,24)=42.74$, $p<0.0001$. Paired 3X CS+: CS1 vs CSn, $p=0.039$; Paired 5X CS+: CS1 vs CSn, $p=0.0005$. $n[\text{Paired 3X}]=8$ and $n[\text{Paired 5X}]=6$ animals.

k) Paired 5X group displayed equivalent conditioned threat response and safety response to CS+ and CS- respectively as paired 3X group during LTM test. Two way ANOVA with Bonferroni's post-hoc test. Effect of pairings: $F(1,24)=0.2942$, $p=0.593$; effect of CS: $F(1,24)=66.46$, $p<0.0001$. $n[\text{Paired 3X}]=8$ and $n[\text{Paired 5X}]=6$ animals.

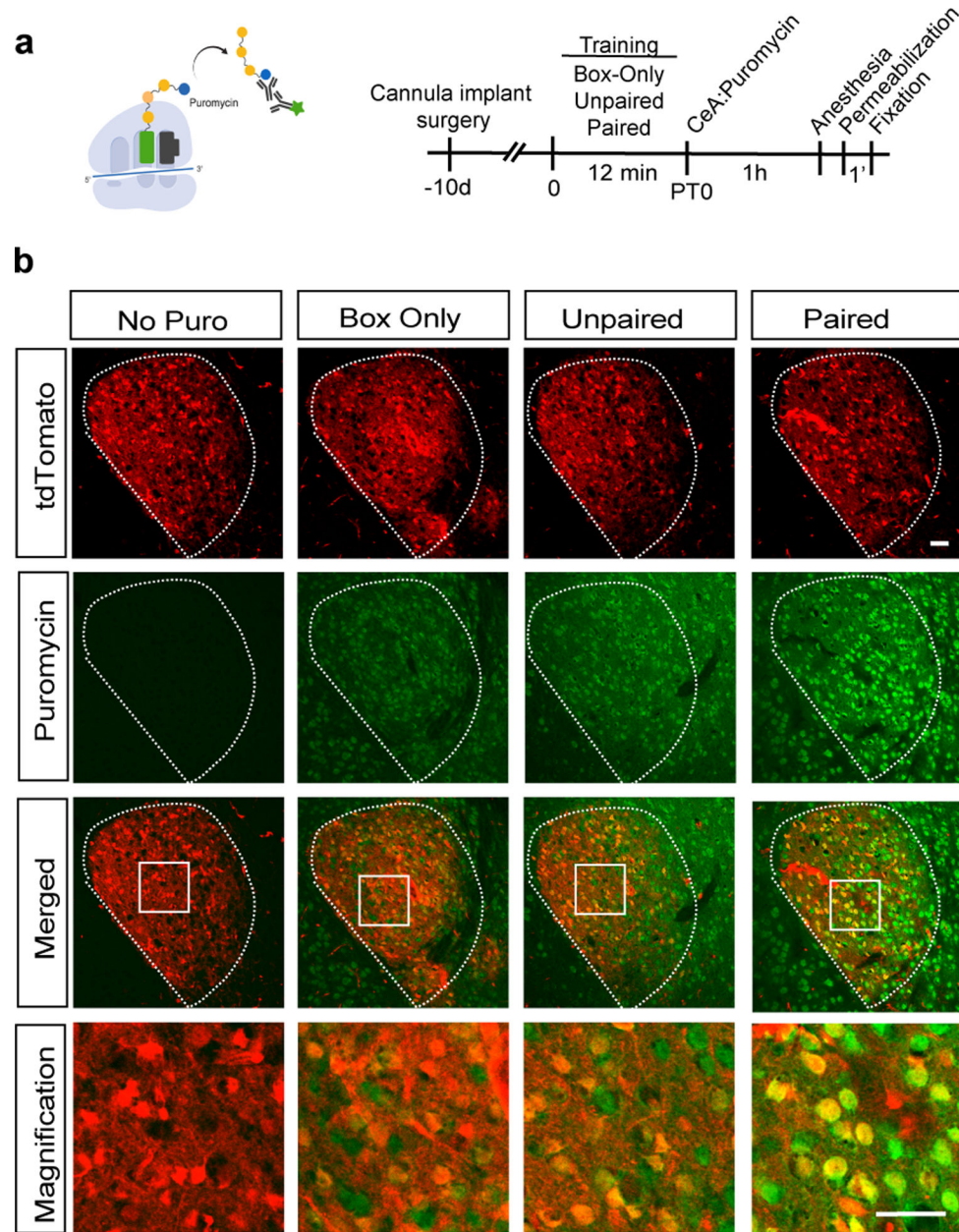
l) Discrimination index for cued threat in Paired 5X group was unaltered compared to Paired 3X group. Unpaired t-test, Two-tailed. $p>0.999$.

Data are presented as mean \pm SEM. * $p<0.05$, ** $p<0.01$, *** $p<0.001$, **** $p<0.0001$. n.s. nonsignificant.



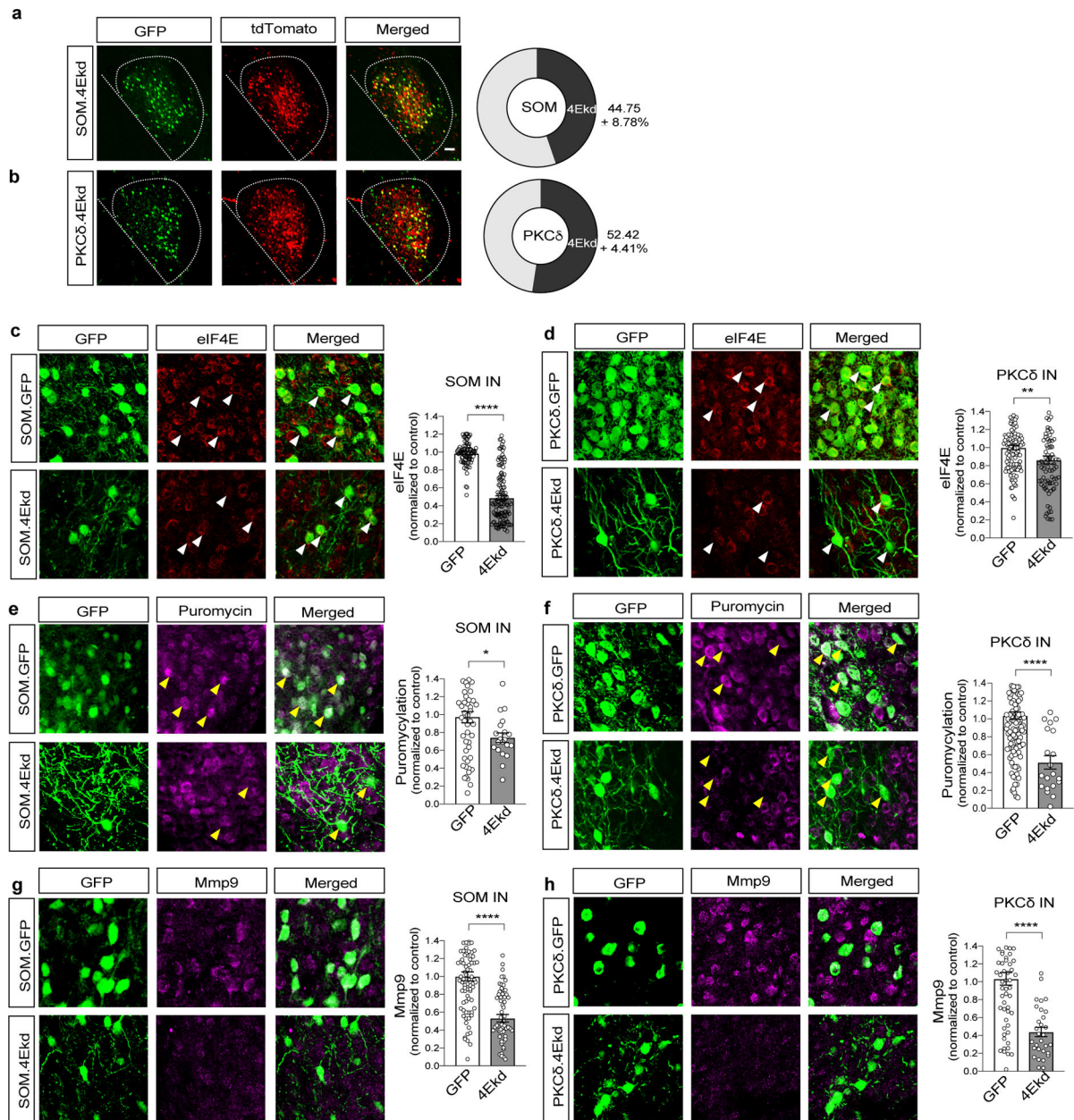
Extended Data Figure 2. Distinct inhibitory neuron subpopulations in centrolateral amygdala.

- a) Co-immunostaining for GFP and neuronal marker, NeuN, in PKC δ .TRAP amygdala sections. 57.96 \pm 2.86% of all neurons in centrolateral amygdala are PKC δ INs. n=3 animals/group.
- b) Co-immunostaining for tdTomato and NeuN in SOM.tdT amygdala sections. SOM INs constitute 55.36 \pm 0.91% of all neurons in CeL. n=3 animals/group.
- c) Immunohistochemistry for PKC δ in SOM.tdT brain sections shows largely non-overlapping expression of PKC δ in SOM Cre expressing cells in CeL.
- d) Immunohistochemistry for SOM in PKC δ .tdT brain sections also shows largely non-overlapping populations but the subcellular distribution of SOM in neuronal processes makes it difficult to analyse the extent of SOM co-expression in PKC δ Cre expressing cell populations.
- e) Multiplexed smFISH for *Prkcd* and *Som* showing mutually exclusive interneurons in CeL expressing these two mRNA populations.
- f) Immunohistochemistry data for PKC δ .TRAP amygdala sections showing expression of p-S6 (S235/6) in PKC δ neurons in CeL across three groups (Box-Only, Unpaired and Paired) at 30 min post training. One-way ANOVA with Bonferroni's post-hoc test. F(2,334)=71.67, p<0.0001. n[Box-Only]=117, n[Unpaired]=118 and n[Paired]=102 cells from 3 animals/group.
- g) Immunohistochemistry data for SOM tdTomato sections showing p-S6 (S235/6) in SOM neurons in CeL across groups. One-way ANOVA with Bonferroni's post-hoc test. F(2,292)=44.18, p<0.0001. n[Box-Only]=162, n[Unpaired]=158 and n[Paired]=165 cells from 3 animals/group. Scale bar, 50 μ m.



Extended Data Figure 3. Differential threat conditioning induces *de novo* translation in CeL neurons.

- a) Schematic for the *in vivo* de novo translation labeling assay with puromycin infusion in central amygdala.
- b) *De novo* translation was upregulated in PKC δ INs in the Paired training group compared to Box-Only and Unpaired controls. Insets show higher magnification.



Extended Data Figure 4. Cell-type-specific knockdown of cap dependent translation in CeL neurons.

- a) Proportion of endogenous SOM.tdT INs chemogenetically targeted to express shmir-eIF4E in a cre- and tet-dependent manner. 44.75±8.78% of SOM.tdT INs in CeL expressed shmir-eIF4E. n=3 animals/group.
- b) Proportion of endogenous PKCδ.tdT INs chemogenetically targeted to express shmir-eIF4E in a cre- and tet-dependent manner. 52.42±4.41% of PKCδ.tdT INs in CeL expressed shmir-eIF4E. n=3 animals/group.
- c) eIF4E level was significantly reduced in SOM INs in SOM.4Ekd group compared to SOM.GFP control. Unpaired t-test, Two-tailed. $p < 0.0001$. n[SOM.GFP]=87 and n[SOM.4Ekd]=132 cells from 3 animals/group.

d) eIF4E level was significantly knocked down in PKC δ INs in PKC δ .4Ekd group compared to PKC δ .GFP control. Unpaired t-test, Two-tailed. $p=0.0056$, $n[\text{PKC}\delta.\text{GFP}]=121$ and $n[\text{PKC}\delta.4\text{Ekd}]=87$ cells from 3 animals/group.

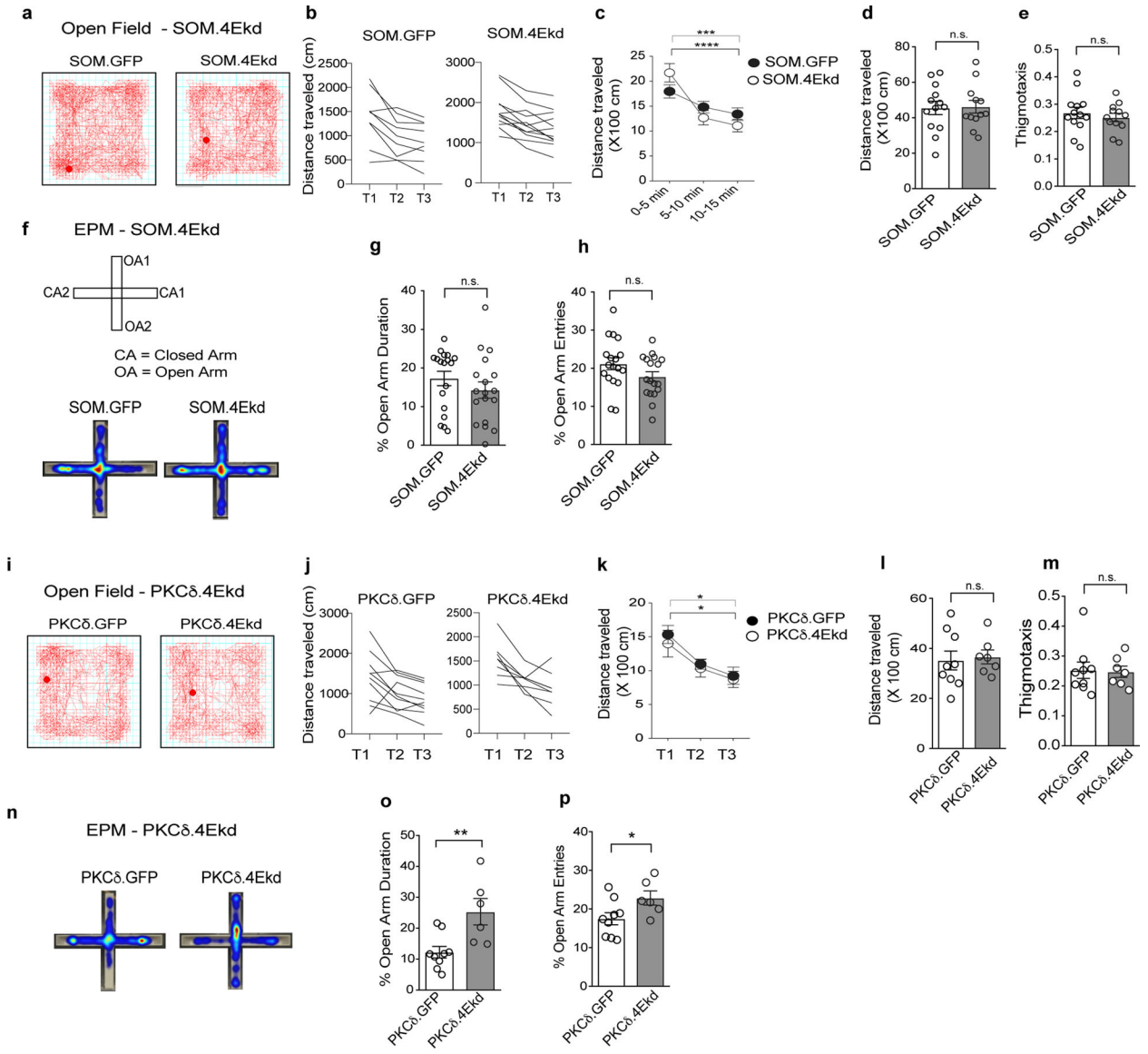
e) Global *de novo* translation, as measured with puromycin assay, was significantly reduced in SOM.4Ekd group compared to control. Unpaired t-test, Two-tailed. $p=0.0363$. $n[\text{SOM.GFP}]=53$ and $n[\text{SOM.4Ekd}]=20$ cells from 3 animals/ group.

f) Similarly, global *de novo* protein synthesis was significantly diminished in PKC δ .4Ekd group compared to control. Unpaired t-test, Two-tailed. $p<0.0001$. $n[\text{PKC}\delta.\text{GFP}]=120$ and $n[\text{PKC}\delta.4\text{Ekd}]=20$ cells from 4 animals/ group.

e) MMP9 levels was significantly reduced in SOM.4Ekd mice compared to control. Unpaired t-test, Two-tailed. $p<0.0001$. $n[\text{SOM.GFP}]=87$ and $n[\text{SOM.4Ekd}]=60$ cells from 3 animals/group.

f) Similarly, MMP9 level was significantly reduced in PKC δ .4Ekd group compared to control. Unpaired t-test, Two-tailed. $p<0.0001$. $n[\text{PKC}\delta.\text{GFP}]=60$ and $n[\text{PKC}\delta.4\text{Ekd}]=30$ cells from 3 animals/group.

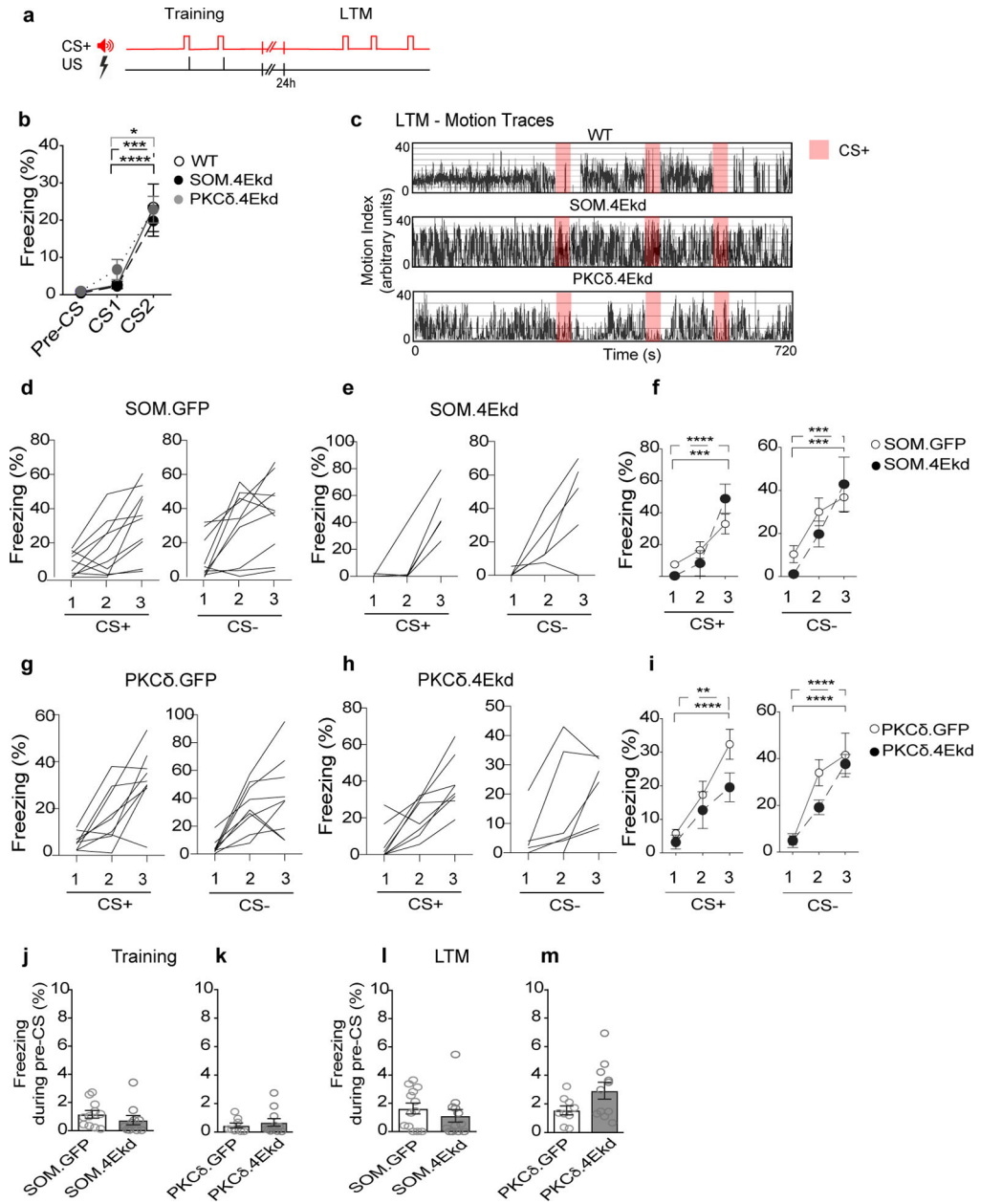
Data are presented as mean \pm SEM. * $p<0.05$, ** $p<0.01$, *** $p<0.001$, **** $p<0.0001$. n.s. nonsignificant. Scale bar, 50 μm .



Extended Data Figure 5. Inhibition of cap-dependent translation and anxiety related behaviors.

- a) Representative open field activity traces for SOM.GFP and SOM.4Ekd animals.
- b) Distance traveled in the open field arena for individual SOM.GFP and SOM.4Ekd animals.
- c) XY plot showing normal acclimation of SOM.GFP and SOM.4Ekd animals to the open field arena. Effect of Time: $F(2,46)=45.50$, $p<0.0001$. $n[\text{SOM.GFP}]=13$ and $n[\text{SOM.4Ekd}]=12$ animals.
- d) SOM.GFP and SOM.4Ekd animals display equivalent spontaneous locomotion in the open field arena. Unpaired t-test, Two-tailed. $p=0.895$. $n[\text{SOM.GFP}]=13$ and $n[\text{SOM.4Ekd}]=12$ animals.
- e) SOM.4Ekd mice display normal thigmotaxis behavior compared to control. Unpaired t-test, Two-tailed. $p=0.521$. $n[\text{SOM.GFP}]=13$ and $n[\text{SOM.4Ekd}]=12$ animals.

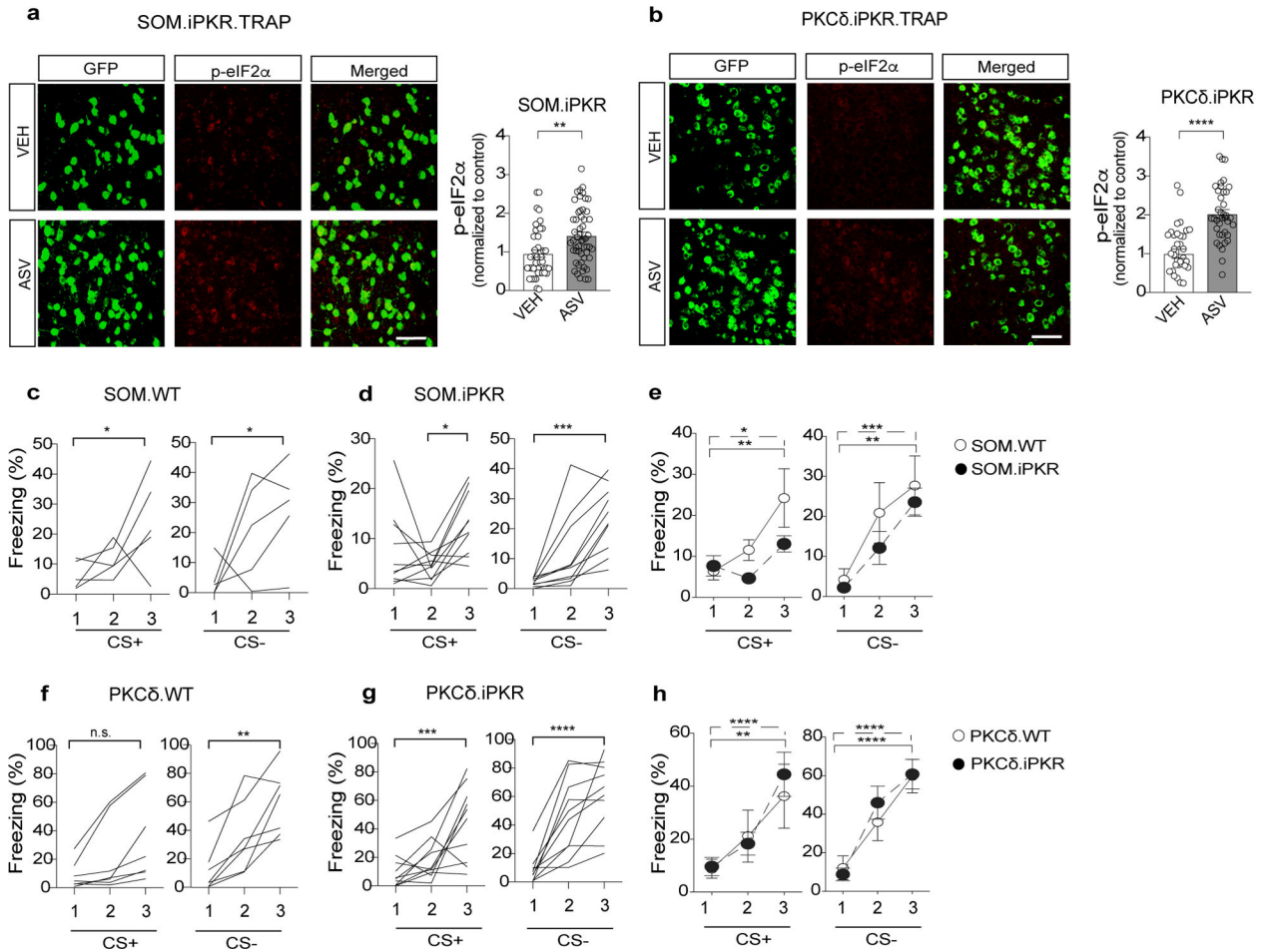
- f) Representative activity heat map in elevated plus maze for SOM.GFP and SOM.4Ekd animals.
- g) SOM.GFP and SOM.4Ekd animals spend similar duration in the open arm, as a percent of total duration. Unpaired t-test, Two-tailed. $p=0.288$. $n[\text{SOM.GFP}]=18$ and $n[\text{SOM.4Ekd}]=18$ animals.
- h) SOM.GFP and SOM.4Ekd mice make equivalent entries into the open arm. Unpaired t-test, Two-tailed. $p=0.107$. $n[\text{SOM.GFP}]=18$ and $n[\text{SOM.4Ekd}]=18$ animals.
- i) Representative open field activity traces for PKC δ .GFP and PKC δ .4Ekd animals.
- j) Distance traveled in the open field arena for individual PKC δ .GFP and PKC δ .4Ekd animals.
- k) XY plot showing normal acclimation of PKC δ .GFP and PKC δ .4Ekd animals to the open field arena. RM Two-way ANOVA. Time: $F(2,32)=19.12$, $p<0.0001$. $n[\text{PKC}\delta.\text{GFP}]=10$ and $n[\text{PKC}\delta.\text{4Ekd}]=8$ animals.
- l) Bar plot showing total distance traveled by PKC δ WT and PKC δ 4Ekd mice in the open field arena. Unpaired t-test, Two-tailed. $p=0.772$. $n[\text{PKC}\delta.\text{GFP}]=10$ and $n[\text{PKC}\delta.\text{4Ekd}]=8$ animals.
- m) PKC δ .4Ekd mice show normal thigmotaxis in the open field arena compared to PKC δ .GFP control. Unpaired t-test, Two-tailed. $p=0.888$. $n[\text{PKC}\delta.\text{GFP}]=7$ and $n[\text{PKC}\delta.\text{4Ekd}]=9$ animals.
- n) Representative activity heat maps in elevated plus maze for PKC δ .GFP and PKC δ .4Ekd animals.
- o) Bar plot showing significantly increased %time spent in the open arm for PKC δ .4Ekd animals compared to PKC δ .GFP controls. Unpaired t-test, Two-tailed. $p=0.0074$. $n[\text{PKC}\delta.\text{GFP}]=9$ and $n[\text{PKC}\delta.\text{4Ekd}]=6$ animals.
- p) Bar plot showing % entries into the open arm for PKC δ .4Ekd animals compared to PKC δ .GFP controls. $p=0.0476$. $n[\text{PKC}\delta.\text{GFP}]=9$ and $n[\text{PKC}\delta.\text{4Ekd}]=6$ animals.
- Data are presented as mean +SEM. ** $p<0.01$, **** $p<0.0001$, n.s. nonsignificant.



Extended Data Figure 6. Inhibition of cap-dependent translation in CeL INs and simple threat conditioning.

- a) Schematic for simple threat conditioning paradigm in SOM and PKCδ 4Ekd mice.
- b) Normal memory acquisition in simple threat-conditioning in WT, SOM.4Ekd and PKCδ 4Ekd groups. Effect of CS: $F(2,50)=32.28, p<0.0001$. $n[WT]=12, n[SOM.4Ekd]=11$ and $n[PKCδ.4Ekd]=5$ animals.
- c) Representative motion traces for WT, SOM.4Ekd and PKCδ.4Ekd groups during LTM test.
- d) Freezing response to CS+ and CS- in individual SOM.GFP animals during training.
- e) Freezing response to CS+ and CS- in individual SOM.4Ekd animals during training.

- f) Normal memory acquisition in differential threat conditioning in SOM.GFP and SOM.4Ekd mice. Effect of CS+: $F(2,26)=34.66$, $p<0.0001$; effect of CS-: $F(2,26)=20.81$, $p<0.0001$. $n[\text{SOM.GFP}]=10$ and $n[\text{SOM.4Ekd}]=5$ animals.
- g) Freezing response to CS+ and CS- in individual PKC δ .GFP animals during training.
- h) Freezing response to CS+ and CS- in individual PKC δ .4Ekd animals during training.
- i) Normal memory acquisition in PKC δ .GFP and PKC δ .4Ekd mice. Effect of CS+: $F(2,34)=24.67$, $p<0.0001$; effect of CS-: $F(2,34)=36.84$, $p<0.0001$. $n[\text{PKC}\delta.\text{GFP}]=9$ and $n[\text{PKC}\delta.4\text{Ekd}]=10$ animals.
- j) SOM.4Ekd mice have negligible freezing response during pre-CS in Training phase compared to controls. Unpaired t-test, Two-tailed. $p=0.341$. $n[\text{SOM.GFP}]=11$ and $n[\text{SOM.4Ekd}]=10$ animals.
- k) PKC δ .4Ekd mice have negligible freezing response during pre-CS in the Training phase compared to controls. Unpaired t-test, Two-tailed. $p=0.541$. $n[\text{PKC}\delta.\text{GFP}]=8$ and $n[\text{PKC}\delta.4\text{Ekd}]=11$ animals.
- l) SOM.4Ekd mice have comparable low freezing response during pre-CS in LTM test compared to controls. Unpaired t-test, Two-tailed. $p=0.389$. $n[\text{SOM.GFP}]=13$ and $n[\text{SOM.4Ekd}]=12$ animals.
- m) PKC δ .4Ekd mice have comparable low freezing response during pre-CS in LTM test compared to controls. Unpaired t-test, Two-tailed. $p=0.068$. $n[\text{PKC}\delta.\text{GFP}]=9$ and $n[\text{PKC}\delta.4\text{Ekd}]=11$ animals.
- Data are presented as mean +SEM. ** $p<0.01$, **** $p<0.0001$, n.s. nonsignificant.

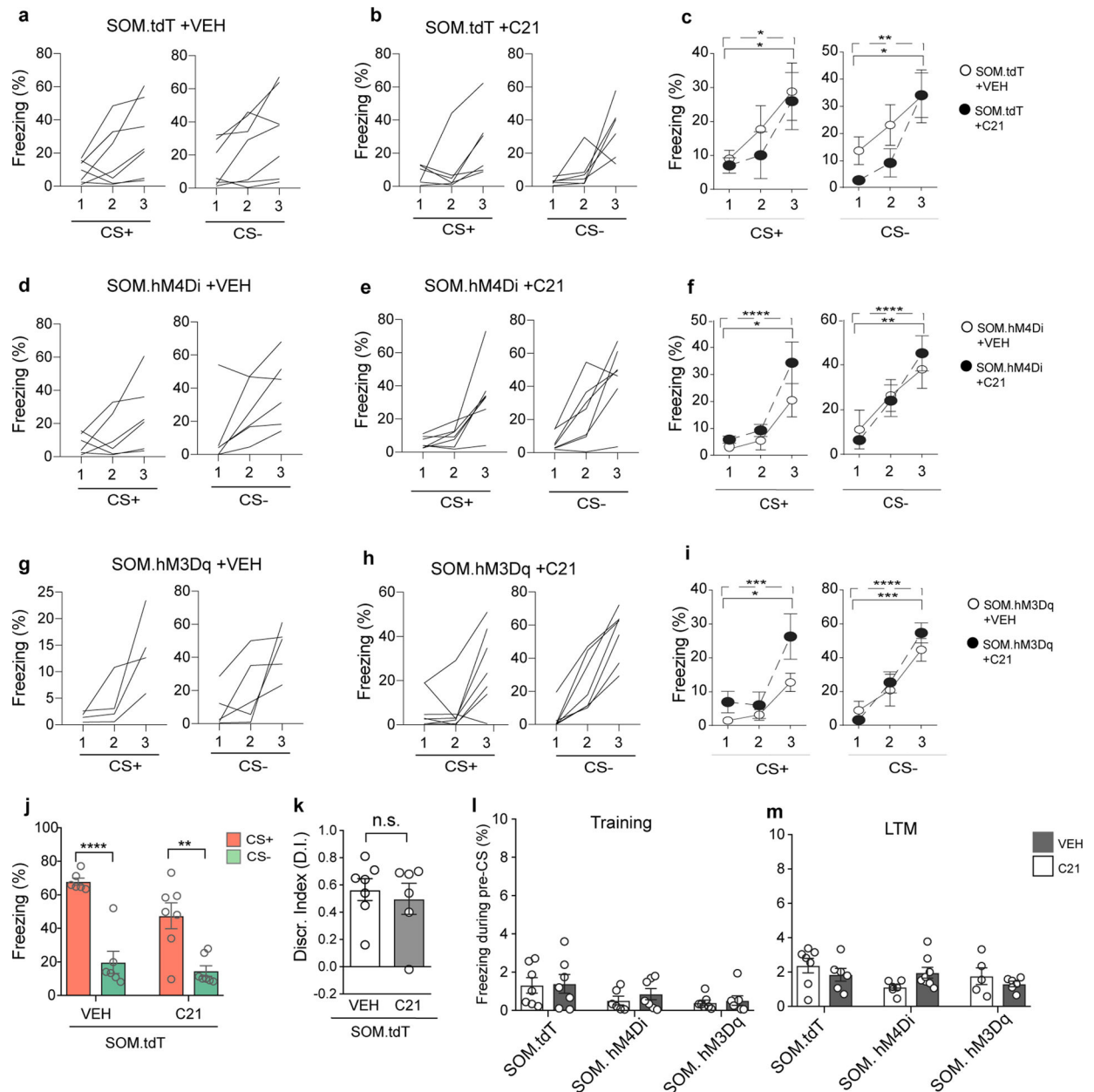


Extended Data Figure 7. Cell type-specific eIF2α phosphorylation and threat conditioning

- a) Compared to vehicle controls, ASV infusion in the central amygdala of SOM.iPKR.TRAP animals significantly increased phosphorylation of eIF2α in SOM neurons. Unpaired t-test, Two-tailed. $p=0.0013$. $n[\text{SOM.iPKR.TRAP +VEH}]=43$ and $n[\text{SOM.iPKR.TRAP +ASV}]=53$ cells from 3 animals/ group.
- b) ASV infusion in CeA of PKCδ.iPKR.TRAP mice also significantly elevated p-eIF2α in PKCδ neurons compared to vehicle control. Unpaired t-test, Two-tailed. $p<0.0001$. $n[\text{PKCδ.iPKR.TRAP +VEH}]=36$ and $n[\text{PKCδ.iPKR.TRAP +ASV}]=38$ cells from 3 animals/ group.
- c) Freezing response to CS+ and CS- in individual SOM.WT animals during training.
- d) Freezing response to CS+ and CS- in individual SOM.iPKR animals during training.
- e) Normal memory acquisition in SOM.WT and SOM.iPKR animals in differential threat conditioning paradigm. RM Two-way ANOVA with Bonferroni's post-hoc test. Effect of CS +: $F(2,26)=10.98$, $p=0.0003$; effect of CS-: $F(2,26)=18.40$, $p<0.0001$. $n[\text{SOM.WT}]=5$ and $n[\text{SOM.iPKR}]=10$ animals.
- f) Freezing response to CS+ and CS- in individual PKCδ.WT animals during training.
- g) Freezing response to CS+ and CS- in individual PKCδ.iPKR animals during training.
- h) Normal memory acquisition in PKCδ.WT and PKCδ.iPKR animals in differential threat conditioning paradigm. RM Two-way ANOVA with Bonferroni's post-hoc test. Effect of CS

+: $F(2,30)=18.70$, $p<0.0001$; effect of CS-: $F(2,30)=46.39$, $p<0.0001$. $n[\text{PKC.WT}]=7$ and $n[\text{PKC.iPKR}]=10$ animals.

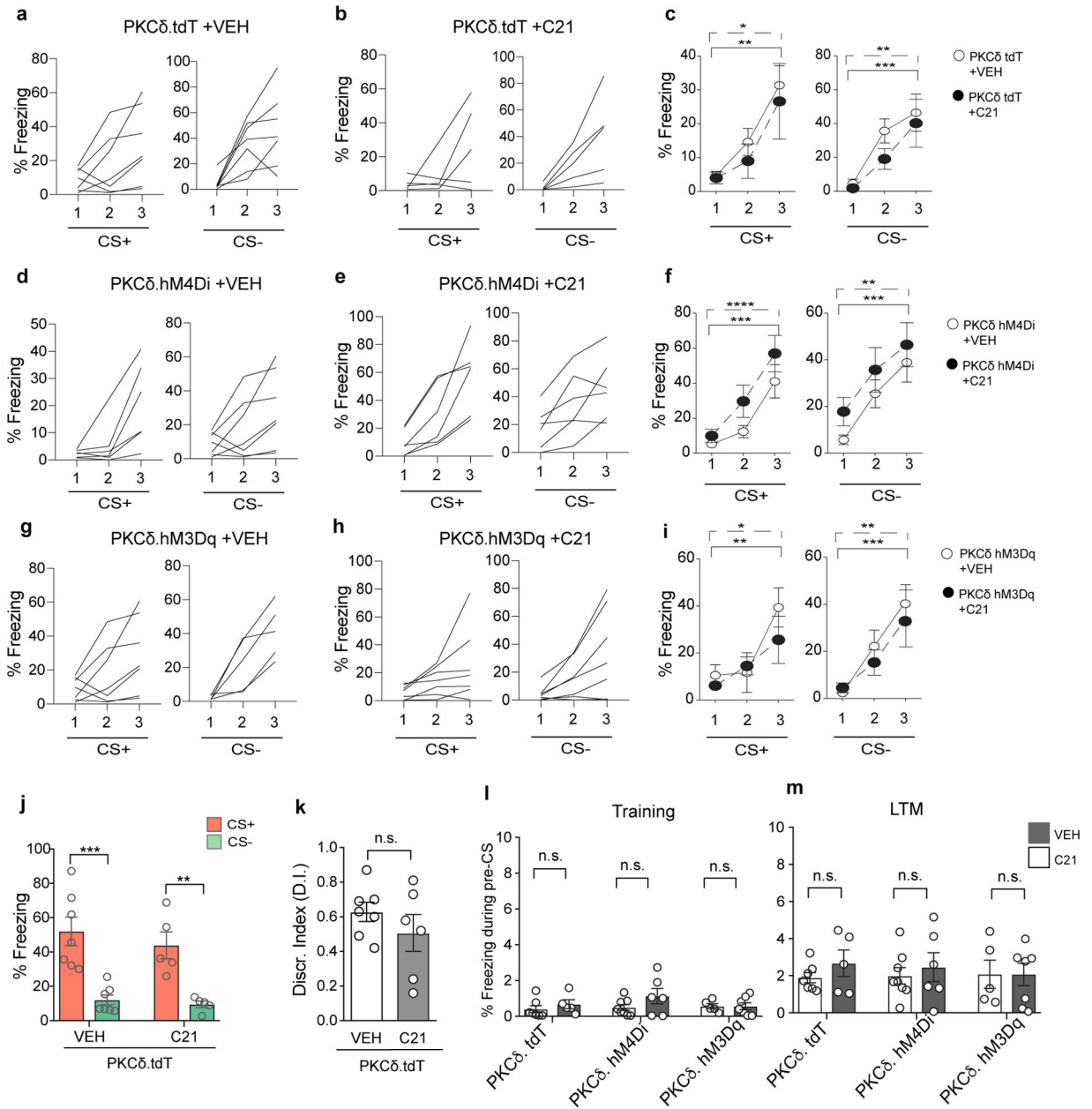
Data are presented as mean \pm SEM. ** $p<0.01$, **** $p<0.0001$. Scale bar, 50 μm .



Extended Data Figure 8. Chemogenetic modulation of G-protein signaling in CeL SOM INs affects associative learning.

- a) Freezing response to CS+ and CS- in individual SOM.tdT animals treated with vehicle during training.
- b) Freezing response to CS+ and CS- in individual SOM.tdT animals treated with C21 during training.

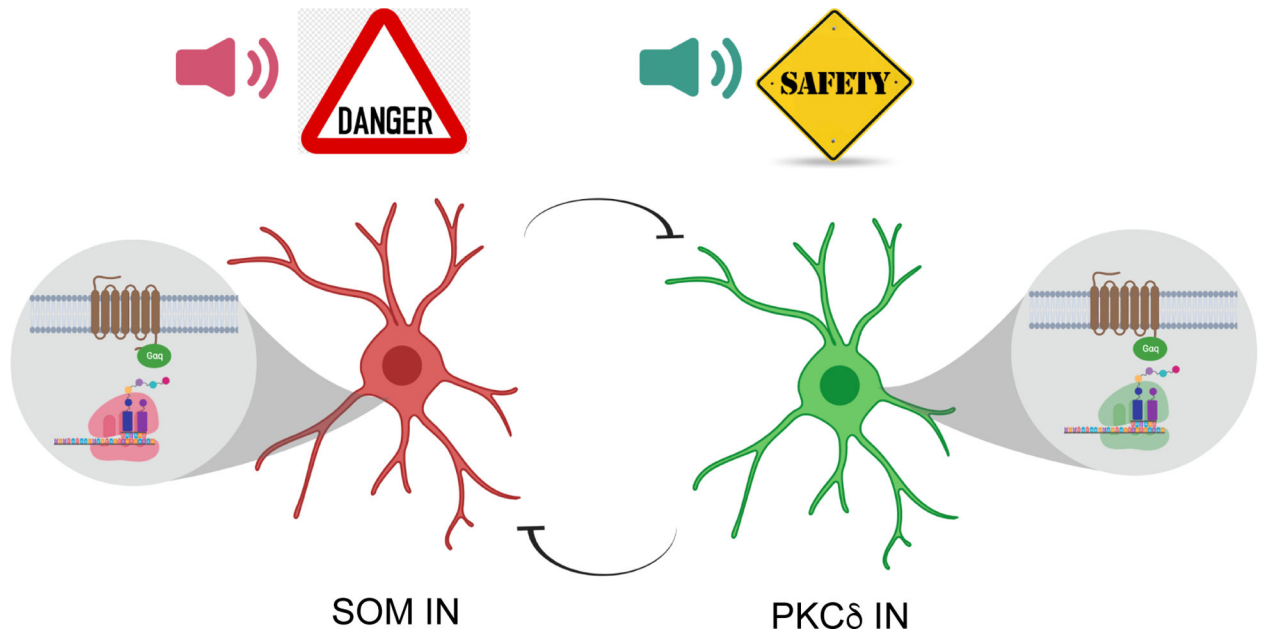
-) C21 treated SOM.tdT mice learn normally compared to VEH treated controls. RM Two-way ANOVA with Bonferroni's post-hoc test. Effect of CS+: $F(2,22)=8.02$, $p=0.0024$; effect of CS-: $F(2,22)=17.00$, $p<0.0001$. $n[\text{SOM.tdT +VEH}]=7$ and $n[\text{SOM.tdT +C21}]=6$ animals.
- d) Freezing response to CS+ and CS- in individual SOM.hM4Di animals treated with vehicle during training.
- e) Freezing response to CS+ and CS- in individual SOM.hM4Di animals treated with C21 during training.
- f) C21 treated SOM.hM4Di mice have normal memory acquisition relative to VEH controls. RM Two-way ANOVA with Bonferroni's post-hoc test. CS+: $F(2,22)=20.62$, $p<0.0001$; CS-: $F(2,22)=19.62$, $p<0.0001$. $n[\text{SOM.hM4Di +VEH}]=6$ and $n[\text{SOM.hM4Di +C21}]=7$ animals.
- g) Freezing response to CS+ and CS- in individual SOM.hM3Dq animals treated with vehicle during training.
- h) Freezing response to CS+ and CS- in individual SOM.hM3Dq animals treated with C21 during training.
- i) C21 treated SOM.hM3Dq animals acquire differential threat memory normally relative to VEH controls. RM Two-way ANOVA with Bonferroni's post-hoc test. Effect of CS+: $F(2,20)=17.09$, $p<0.0001$; effect of CS-: $F(2,20)=38.94$, $p<0.0001$. $n[\text{SOM.hM4Di +VEH}]=5$ and $n[\text{SOM.hM4Di +C21}]=7$ animals.
- j) C21 treated SOM.tdT mice exhibit normal threat and safety LTM response to CS+ and CS- respectively. RM Two-way ANOVA with Bonferroni's post-hoc test. Effect of drug: $F(1,22)=5.233$, $p=0.0321$; effect of CS: $F(1,22)=52.87$, $p<0.0001$. $n[\text{SOM.tdT +VEH}]=7$ and $n[\text{SOM.tdT +C21}]=6$ animals.
- k) C21 treatment does not alter cued threat discrimination index in SOM.tdT mice. Unpaired t-test, Two-tailed. $p=0.6313$. $n[\text{SOM.tdT +VEH}]=7$ and $n[\text{SOM.tdT +C21}]=6$ animals.
- l) Freezing response during pre-CS of training session is negligible across all C21 and VEH treated SOM groups. Two-way ANOVA. Effect of drug: $F(2,31)=2.410$, $p=0.1064$. $n[\text{SOM.tdT +VEH}]=7$, $n[\text{SOM.tdT +C21}]=6$, $n[\text{SOM.hM4Di +VEH}]=6$, $n[\text{SOM.hM4Di +C21}]=7$, $n[\text{SOM.hM3Dq +VEH}]=4$ and $n[\text{SOM.hM3Dq +C21}]=7$ animals.
- m) C21 treated SOM.tdT, SOM.hM4Di and SOM.hM3Dq mice have equivalent freezing response during pre-CS of LTM test compared to VEH controls. Two-way ANOVA. Effect of drug: $F(2,32)=1.899$, $p=0.1663$. $n[\text{SOM.tdT +VEH}]=7$, $n[\text{SOM.tdT +C21}]=6$, $n[\text{SOM.hM4Di +VEH}]=6$, $n[\text{SOM.hM4Di +C21}]=8$, $n[\text{SOM.hM3Dq +VEH}]=5$ and $n[\text{SOM.hM3Dq +C21}]=6$ animals.
- Data are presented as mean \pm SEM. * $p<0.05$, ** $p<0.01$, *** $p<0.001$, **** $p<0.0001$. n.s. nonsignificant.



Extended Data Figure 9. Chemogenetic modulation of G-protein signaling in CeL PKC δ INs affects associative learning.

- a) Freezing response to CS+ and CS- in individual PKC δ .tdT animals treated with vehicle during training.
- b) Freezing response to CS+ and CS- in individual PKC δ .tdT animals treated with C21 during training.
- c) C21 treated PKC δ .tdT animals have normal memory acquisition relative to VEH controls, with progressive increase in freezing response to successive presentation of CS's. RM Two-way ANOVA with Bonferroni's post-hoc test. Effect of CS+: $F(2,20)=12.22$, $p=0.0003$; effect of CS-: $F(2,20)=18.65$, $p<0.0001$. $n[\text{PKC}\delta.\text{tdT} + \text{VEH}]=7$ and $n[\text{PKC}\delta.\text{tdT} + \text{C21}]=5$ animals.

- d) Freezing response to CS+ and CS- in individual PKC δ .hM4Di animals treated with vehicle during training.
- e) Freezing response to CS+ and CS- in individual PKC δ .hM4Di animals treated with C21 during training.
- f) C21 treated PKC δ .hM4Di animals learn normally compared to VEH controls. RM Two-way ANOVA with Bonferroni's post-hoc test. Effect of CS+: $F(2,24)=29.92$, $p<0.0001$; effect of CS-: $F(2,24)=19.58$, $p<0.0001$. $n[\text{PKC}\delta.\text{hM4Di} + \text{VEH}]=8$ and $n[\text{PKC}\delta.\text{hM4Di} + \text{C21}]=6$ animals.
- g) Freezing response to CS+ and CS- in individual PKC δ .hM3Dq animals treated with vehicle during training.
- h) Freezing response to CS+ and CS- in individual PKC δ .hM3Dq animals treated with C21 during training.
- i) C21 treated PKC δ .hM3Dq animals acquire differential threat memory normally compared to VEH controls. RM Two-way ANOVA with Bonferroni's post-hoc test. Effect of CS+: $F(2,20)=15.90$, $p<0.0001$; effect of CS-: $F(2,20)=20.67$, $p<0.0001$. $n[\text{PKC}\delta.\text{hM3Dq} + \text{VEH}]=5$ and $n[\text{PKC}\delta.\text{hM3Dq} + \text{C21}]=7$ animals.
- j) C21 treated PKC δ .tdT mice exhibit normal threat and safety LTM response to CS+ and CS- respectively. RM Two-way ANOVA with Bonferroni's post-hoc test. Effect of CS: $F(1,20)=0.402$. $n[\text{PKC}\delta.\text{tdT} + \text{VEH}]=7$ and $n[\text{PKC}\delta.\text{tdT} + \text{C21}]=5$ animals.
- k) C21 treatment does not alter cued threat discrimination index in PKC δ .tdT mice. Unpaired t-test, Two-tailed. $p=0.3116$. $n[\text{PKC}\delta.\text{tdT} + \text{VEH}]=7$ and $n[\text{PKC}\delta.\text{tdT} + \text{C21}]=6$ animals.
- l) Freezing response during pre-CS of the training session is negligible across all C21 and VEH treated PKC δ groups. Two-way ANOVA. Effect of drug: $F(2,35)=0.2326$, $p=0.794$. $n[\text{PKC}\delta.\text{tdT} + \text{VEH}]=7$, $n[\text{PKC}\delta.\text{tdT} + \text{C21}]=6$, $n[\text{PKC}\delta.\text{hM4Di} + \text{VEH}]=8$, $n[\text{PKC}\delta.\text{hM4Di} + \text{C21}]=6$, $n[\text{PKC}\delta.\text{hM3Dq} + \text{VEH}]=5$ and $n[\text{PKC}\delta.\text{hM3Dq} + \text{C21}]=7$ animals.
- m) C21 treatment in PKC δ .tdT, PKC δ .hM4Di and PKC δ .hM3Dq animals does not alter baseline freezing response during pre-CS of LTM test. Two-way ANOVA. Effect of drug: $F(2,32)=0.0171$, $p=0.983$. $n[\text{PKC}\delta.\text{tdT} + \text{VEH}]=7$, $n[\text{PKC}\delta.\text{tdT} + \text{C21}]=5$, $n[\text{PKC}\delta.\text{hM4Di} + \text{VEH}]=8$, $n[\text{PKC}\delta.\text{hM4Di} + \text{C21}]=6$, $n[\text{PKC}\delta.\text{hM3Dq} + \text{VEH}]=5$ and $n[\text{PKC}\delta.\text{hM3Dq} + \text{C21}]=7$ animals.
- Data are presented as mean \pm SEM. * $p<0.05$, ** $p<0.01$, *** $p<0.001$, **** $p<0.0001$. n.s. nonsignificant.

**Extended Data Figure 10.**

Working model of simultaneous consolidation and storage of threat and safety cue-associated memories in CeL SOM and PKC δ INs, respectively.

Supplementary Material

Refer to Web version on PubMed Central for supplementary material.

ACKNOWLEDGEMENTS

We thank Alicia Nnenna Chime and Shantal Taveras for technical assistance. We thank Dr. David Anderson (Caltech) for providing PKC δ :: GluCl α -iCre BAC transgenic mice and Hongkui Zeng (Allen Institute for Brain Science) for providing pAAV.CAG Pr.DIO.tTA plasmid. We thank all members of Klann lab for critical feedback and discussions. We are grateful to Dr. Joseph Ledoux and Rodrigo Del Triano for helpful feedback on this work. This study was supported by National Institute of Health grants NS034007 and NS047384 to E.K., Canadian Institute of Health Research FDN-148366 to J.P and NARSAD Young Investigator grant 26696 to P.S. N.H. is supported by the Howard Hughes Medical Investigator grant.

REFERENCES

1. Fendt M, & Fanselow MS The neuroanatomical and neurochemical basis of conditioned fear. *Neurosci Biobehav Rev* 23:743–760. (1999) [PubMed: 10392663]
2. Pavlov IP Conditioned reflexes. New York, Dover (1927)
3. Rescorla RA Pavlovian conditioned inhibition. *Psychol Bull* 72: 77–94 (1969)
4. Christianson JP, Fernando ABP, Kazama AM, Jovanovic T, Ostroff LE, & Sangha S Inhibition of fear by learned safety signals: minisymposium review. *J Neurosci* 32(41): 14118–14124 (2012) [PubMed: 23055481]
5. Jovanovic T et al. Impaired fear inhibition is a biomarker of PTSD but not depression. *Depress Anxiety* 27(3): 244–251 (2010) [PubMed: 20143428]
6. Wilensky AE, Schafe GE, Kristensen MP, & Ledoux JE Rethinking the fear circuit: The central nucleus of the amygdala is required for the acquisition, consolidation, and expression of Pavlovian fear conditioning. *J Neurosci* 26(48): 12387–12396 (2006) [PubMed: 17135400]

7. Ciochhi S et al. Encoding of conditioned fear in central amygdala inhibitory circuits. *Nature* 468: 277–282 (2010) [PubMed: 21068837]
8. Han S et al. Elucidating an affective pain circuit that creates a threat memory. *Cell* 162: 363–374 (2015) [PubMed: 26186190]
9. Haubensak W et al. Genetic dissection of an amygdala microcircuit that gates conditioned fear. *Nature* 468: 270–276 (2010) [PubMed: 21068836]
10. Shrestha P et al. Cell-type-specific drug-inducible protein synthesis inhibition demonstrates that memory consolidation requires rapid neuronal translation. *Nat Neurosci* 23, 281–292 (2020) [PubMed: 31959934]
11. Kandel ER, Dudai Y, & Mayford MP The molecular and systems biology of memory. *Cell* 157: 163–186 (2016)
12. Klann E, & Dever TE Biochemical mechanisms for translational regulation in synaptic plasticity. *Nat Rev Neurosci* 5: 931–942 (2004) [PubMed: 15550948]
13. Costa-Mattioli M et al. eIF2 α phosphorylation bidirectionally regulates the switch from short- to long-term synaptic plasticity and memory. *Cell* 129: 195–206 (2007) [PubMed: 17418795]
14. Kats IR, & Klann E Translating from cancer to the brain: regulation of protein synthesis by eIF4F. *Learn Mem.* 26(9):332–342. (2019) [PubMed: 31416906]
15. Sidrauski C et al. The small molecule ISRIB reverses the effects of eIF2 phosphorylation on translation and stress granule assembly. *eLife* 4:e05033, doi: 10.7554/eLife.05033 (2015)
16. Thoreen CC et al. A unifying model for mTORC1-mediated regulation of mRNA translation. *Nature* 485 (7396): 109–13 (2012) [PubMed: 22552098]
17. Li H et al. Experience-dependent modification of a central amygdala fear circuit. *Nat Neurosci* 16(3): 332–9 (2013) [PubMed: 23354330]
18. Fadok JP et al. A competitive inhibitory circuit for selection of active and passive fear responses. *Nature* 542: 96–100 (2017) [PubMed: 28117439]
19. Yu K, da Silva PG, Albeanu DF, & Li B Central amygdala Somatostatin neurons gate passive and active defensive behaviors. *J Neurosci* 36(24): 6488–6496 (2016) [PubMed: 27307236]
20. Lin C-J et al. Targeting synthetic lethal interactions between Myc and the eIF4F complex impedes tumorigenesis. *Cell Rep* 1(4): 325–333 (2012) [PubMed: 22573234]
21. Dickins RA et al. Probing tumor phenotypes using stable and regulated synthetic microRNA precursors. *Nat Gen* 37(11): 1289–1295 (2005)
22. Gorkiewicz T et al. Matrix metalloproteinase 9 (MMP-9) is indispensable for long term potentiation in the central and basal but not in the lateral nucleus of the amygdala. *Frontiers Cellular Neurosci* 9:73 (2015)
23. Botta P et al. Regulating anxiety with extrasynaptic inhibition. *Nat Neurosci* 18(10): 1493–1500 (2015) [PubMed: 26322928]
24. Guettier J-M et al. A chemical-genetic approach to study G protein regulation of beta cell function in vivo. *Proc Natl Acad Sci* 45(106): 19197–19202 (2009)
25. Zhu PJ et al. Suppression of PKR promotes network excitability and enhanced cognition by interferon mediated disinhibition. *Cell* 147(6): 1384–96 (2011) [PubMed: 22153080]
26. Banko J et al. Behavioral alterations in mice lacking the translation repressor 4E-BP2. *Neurobiol Learn Mem* 87(2): 248–256 (2007) [PubMed: 17029989]
27. Hoeffler CA et al. Inhibition of the interactions between eukaryotic initiation factors 4E and 4G impairs long-term associative memory consolidation but not reconsolidation. *Proc Natl Acad Sci* 8: 3383–3388 (2011)
28. Sharma V et al. eIF2 α -pathway controls memory consolidation via excitatory and somatostatin inhibitory neurons. *Nature* (2020)
29. Laxmi TR, Stork O, & Pape H-C Generalization of conditioned fear and its behavioral expression in mice. *Beh Brain Res* (2003)
30. Ghosh S and Chattarji S Neuronal encoding of the switch from specific to generalized fear. *Nat Neurosci* 18(1): 112–120 (2015) [PubMed: 25436666]

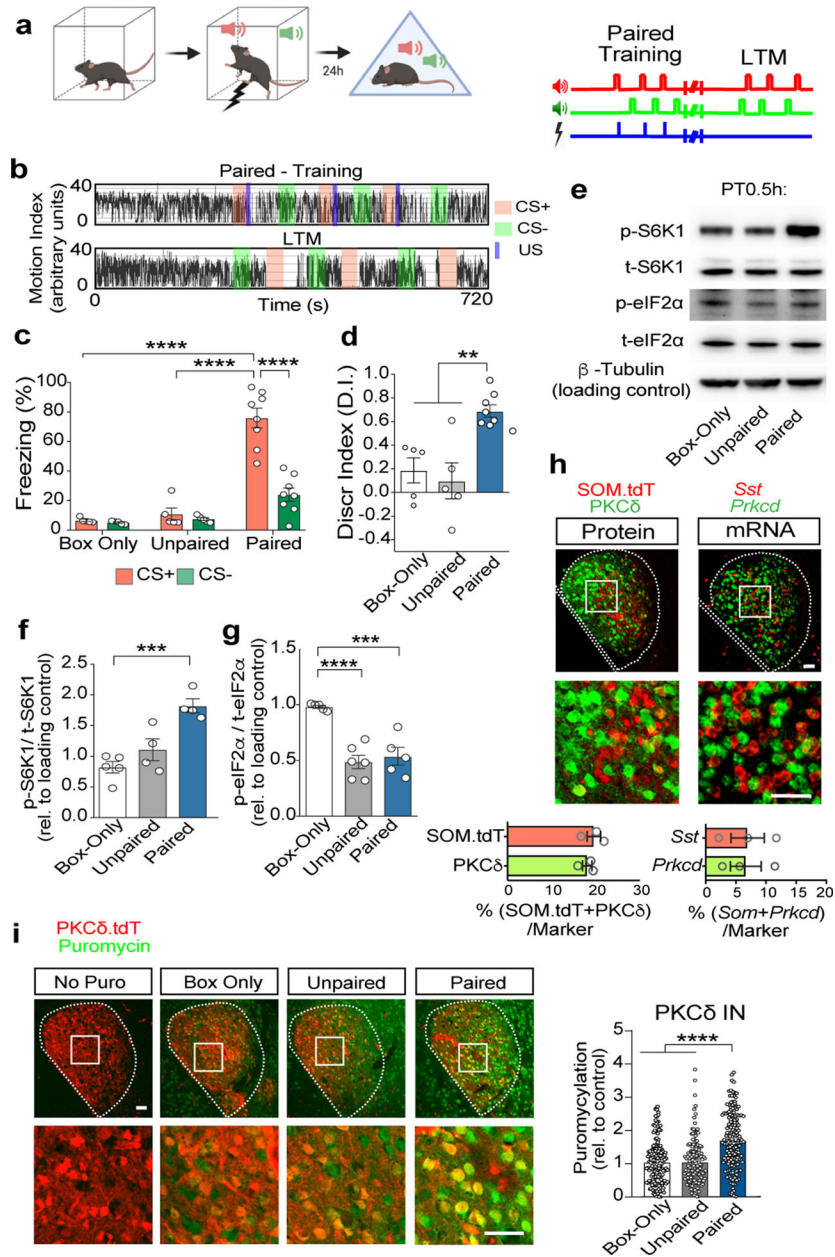


Figure 1. Differential threat-conditioning promotes *de novo* translation in CeL INs.

a) Behavior scheme for differential cued threat-conditioning (left) and tone-shock presentation schedule for the Paired training group (right).

b) Representative motion traces for the Paired group during training and LTM test. CS+ in red block, CS- in green block and US in violet block.

c) During LTM, the Paired group displayed a robust freezing response to CS+ compared to Box-Only and Unpaired groups. Effect of training: $F(2,30)=60.08$, $p<0.0001$, effect of CS: $F(1,30)=22.86$, $p<0.0001$. $n[\text{Box-Only}]=5$, $n[\text{Unpaired}]=5$ and $n[\text{Paired}]=8$ animals.

d) The Paired group exhibited a high discrimination-index for cued threat compared to controls. $F(2,15)=12.01$, $p=0.0008$. $n[\text{Box-Only}]=5$, $n[\text{Unpaired}]=5$ and $n[\text{Paired}]=8$ animals.

- e) Representative immunoblots for mTORC1 and eIF2 pathway indicators: p-S6K1 (T389), t-S6K1, p-eIF2 α (S51), t-eIF2 α and β -Tubulin.
- f) p-S6K1 (T389) was significantly elevated in amygdala lysate of the Paired group compared to the Box-Only control. $F(2,10)=16.41$, $p=0.0007$. $n[\text{Box-Only}]=5$, $n[\text{Unpaired}]=4$ and $n[\text{Paired}]=4$ animals.
- g) Dephosphorylation of eIF2 α (S51) occurred in both Unpaired and Paired groups (right). $F(2,13)=20.94$, $p<0.0001$. $n[\text{Box-Only}]=5$, $n[\text{Unpaired}]=6$ and $n[\text{Paired}]=5$ animals.
- h) Immunostaining for PKC δ in SOM.tdT mice revealed largely distinct cell populations. 18.06% of PKC δ + neurons co-expressed SOM.tdT whereas 19.56% of SOM.tdT neurons co-expressed PKC δ . $n=3$ animals/group (left). smFISH for *Prkcd* and *Sst* mRNAs reveals that double positive cells constitute 6.63% of *Prkcd*+ cells and 6.94% of *Sst*+ cells. $n = 3$ animals/ group (right).
- i) *De novo* translation was significantly upregulated in PKC δ INs in the Paired training group compared to controls. Insets show higher magnification. $F(2,482)=44.18$, $p<0.0001$. $n[\text{Box-Only}]=162$, $n[\text{Unpaired}]=158$ and $n[\text{Paired}]=165$ cells from 3 animals/ group. Statistical tests: Two-way ANOVA with Bonferroni's post-hoc test (c), One-way ANOVA with Bonferroni's post-hoc test (c, f, g, i). Data are presented as mean \pm SEM. * $p<0.05$, ** $p<0.01$, *** $p<0.001$, **** $p<0.0001$. Scale bar, 50 μm .

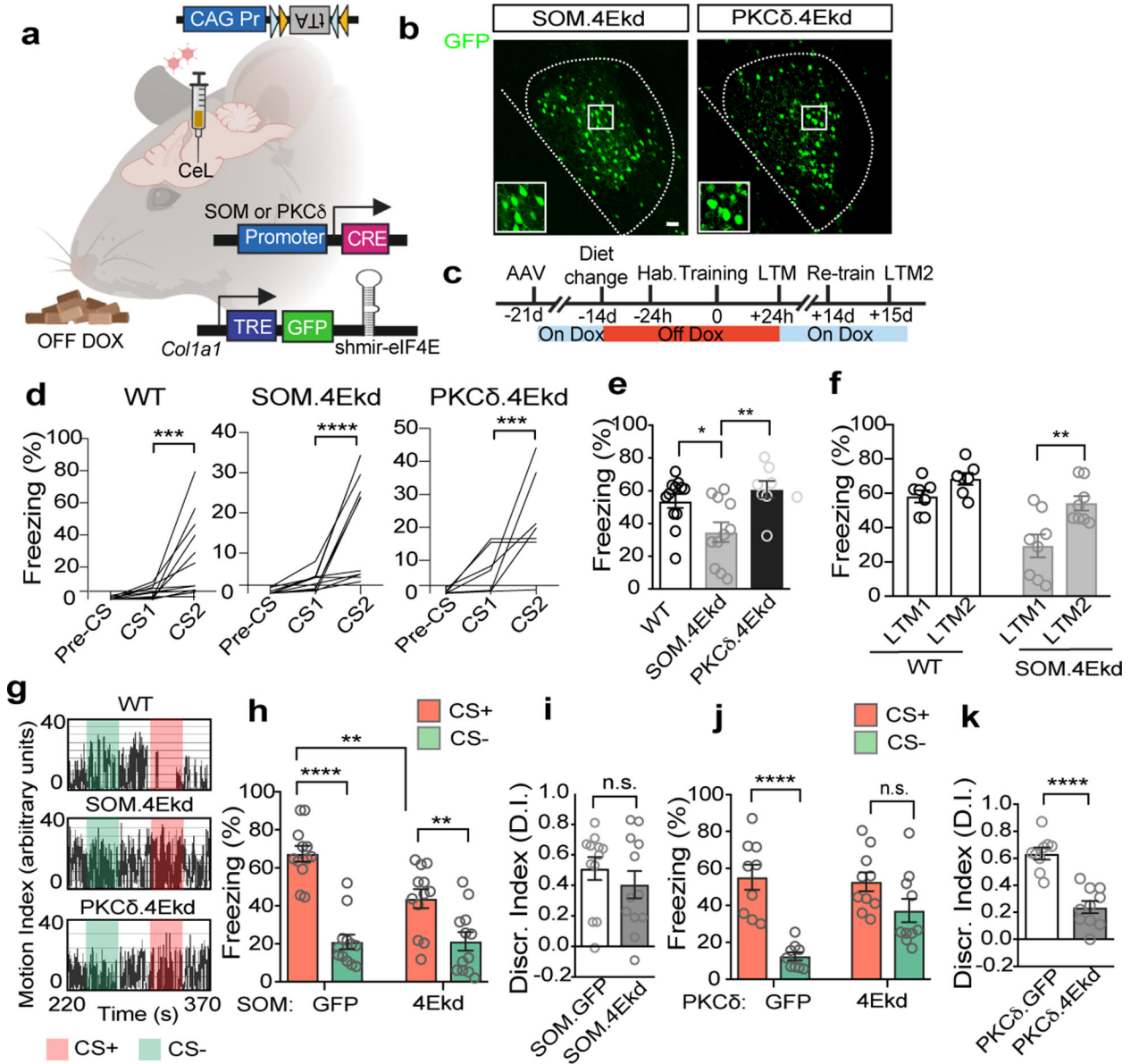


Figure 2. Cell type-specific inhibition of cap-dependent translation in CeL INs.

- Intersectional chemogenetic strategy for knocking down eIF4E in CeL INs.
- Brain region- and cell-type specific expression of GFP.shmir-eIF4E in CeL SOM and PKCδ INs. Insets show higher magnification.
- Behavior paradigm for simple and differential cued threat-conditioning.
- Normal memory acquisition in simple threat-conditioning in WT, SOM.4Ekd and PKCδ.4Ekd groups. WT: $F(2,33)=10.44$, $p=0.0003$, SOM.4Ekd: $F(2,30)=16.26$, $p<0.0001$ and PKCδ.4Ekd: $F(2,21)=13.46$, $p=0.0002$. $n[WT]=12$, $n[SOM.4Ekd]=11$ and $n[PKCδ.4Ekd]=8$ animals.
- SOM.4Ekd mice display significantly impaired LTM compared to both WT and PKCδ 4Ekd mice. $F(2,28)=6.41$, $p=0.0051$. $n[WT]=12$, $n[SOM.4Ekd]=11$ and $n[PKCδ.4Ekd]=8$ animals.

- f) Re-training SOM.4Ekd mice after placing on Dox diet for 14 days rescued the memory deficit. Effect of drug: $F(1,13)=12.33$, $p=0.0038$; effect of genotype: $F(1,13)=21.13$, $p=0.0005$. $n[\text{WT}]=7$ and $n[\text{SOM.4Ekd}]=8$ animals.
- g) Representative motion traces during differential threat LTM test for WT, SOM.4Ekd and PKC δ 4Ekd animals.
- h) SOM.4Ekd mice are significantly impaired in CS+ threat LTM compared to SOM.GFP control, but show equivalent safety response to CS-. Effect of genotype: $F(1,44)=6.68$, $p=0.013$; effect of CS: $F(1,44)=58.41$, $p<0.0001$. $n[\text{SOM.GFP}]=12$ and $n[\text{SOM.4Ekd}]=12$ animals.
- i) Normal cue discrimination-index for SOM.4Ekd mice compared to controls. $p=0.377$.
- j) PKC δ .4Ekd mice are significantly impaired in safety LTM to CS- despite showing comparable threat LTM to CS+. Effect of genotype: $F(1,34)=4.17$, $p=0.049$; effect of CS: $F(1,34)=28.60$, $p<0.0001$. $n[\text{PKC}\delta.\text{GFP}]=9$ and $n[\text{PKC}\delta.4\text{Ekd}]=10$ animals.
- k) Discrimination-index for cued threat is significantly impaired in PKC δ .4Ekd mice compared with PKC δ .GFP controls. $p<0.0001$. $n[\text{PKC}\delta.\text{GFP}]=9$ and $n[\text{PKC}\delta.4\text{Ekd}]=10$ animals.
- Statistical tests: RM One-way ANOVA with Bonferroni's post-hoc test (d, f), One-way ANOVA with Bonferroni's post-hoc test (e), Two-way ANOVA with Bonferroni's post-hoc test (h, j) and Unpaired t-test, two-tailed (i, k). Data are presented as mean \pm SEM. * $p<0.05$, ** $p<0.01$, *** $p<0.001$, **** $p<0.0001$. n.s. nonsignificant. Scale bar, 50 μm .

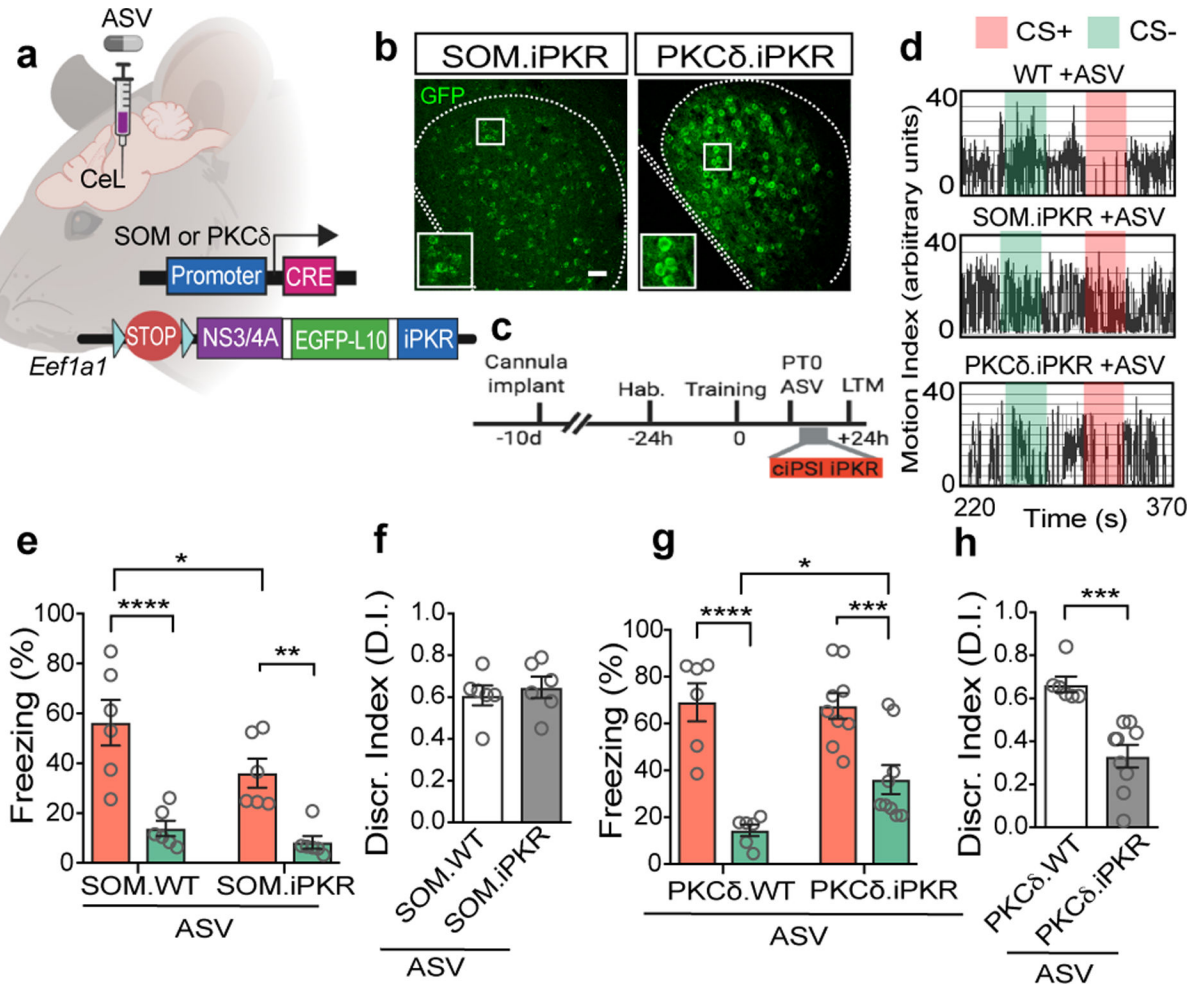


Figure 3. Blocking eIF2-dependent translation in specific CeL INs impairs consolidation of differential threat memories.

a) Chemogenetic strategy for drug-inducible, cell type-specific phosphorylation of eIF2α in SOM and PKCδ INs in CeL.

b) EGFP-L10 expression in SOM.iPKR and PKCδ.iPKR CeL. Insets show higher magnification.

c) Behavior paradigm for differential cued threat-conditioning with temporally precise protein synthesis inhibition during initial consolidation.

d) Representative LTM motion traces for WT +ASV, SOM.iPKR +ASV and PKCδ.iPKR +ASV animals.

e) Intra-CeL infusion of ASV decreased threat-response to CS+ in SOM.iPKR animals while sparing the conditioned safety response to CS-. Effect of genotype: $F(1,20)=4.90$, $p=0.0376$; effect of CS: $F(1,20)=36.78$, $p<0.0001$. $n[\text{SOM.WT +ASV}]=6$ and $n[\text{SOM.iPKR +ASV}]=6$ animals.

f) Normal discrimination-index for cued threat in SOM WT and SOM.iPKR animals. $p=0.595$. $n[\text{SOM.WT +ASV}]=6$ and $n[\text{SOM.iPKR +ASV}]=6$ animals.

g) Intra-CeL infusion of ASV in PKC δ .iPKR mice did not affect the threat-response to CS+ but significantly impaired the safety response to CS-. Effect of CS: $F(1,26)=48.85$, $p<0.0001$. $n[\text{PKC}\delta.\text{WT} + \text{ASV}]=6$ and $n[\text{PKC}\delta.\text{iPKR} + \text{ASV}]=9$ animals.

h) Discrimination-index for cued threat was significantly impaired in PKC δ .iPKR +ASV animals compared to controls. $p=0.0005$. $n[\text{PKC}\delta.\text{WT} + \text{ASV}]=6$ and $n[\text{PKC}\delta.\text{iPKR} + \text{ASV}]=9$ animals.

Statistical tests: Two-way ANOVA with Bonferroni's post-hoc test (e, g) and Unpaired t-test (f, h). Data are presented as mean \pm SEM. * $p<0.05$, ** $p<0.01$, *** $p<0.001$, **** $p<0.0001$. n.s. nonsignificant. Scale bar, 50 μm .

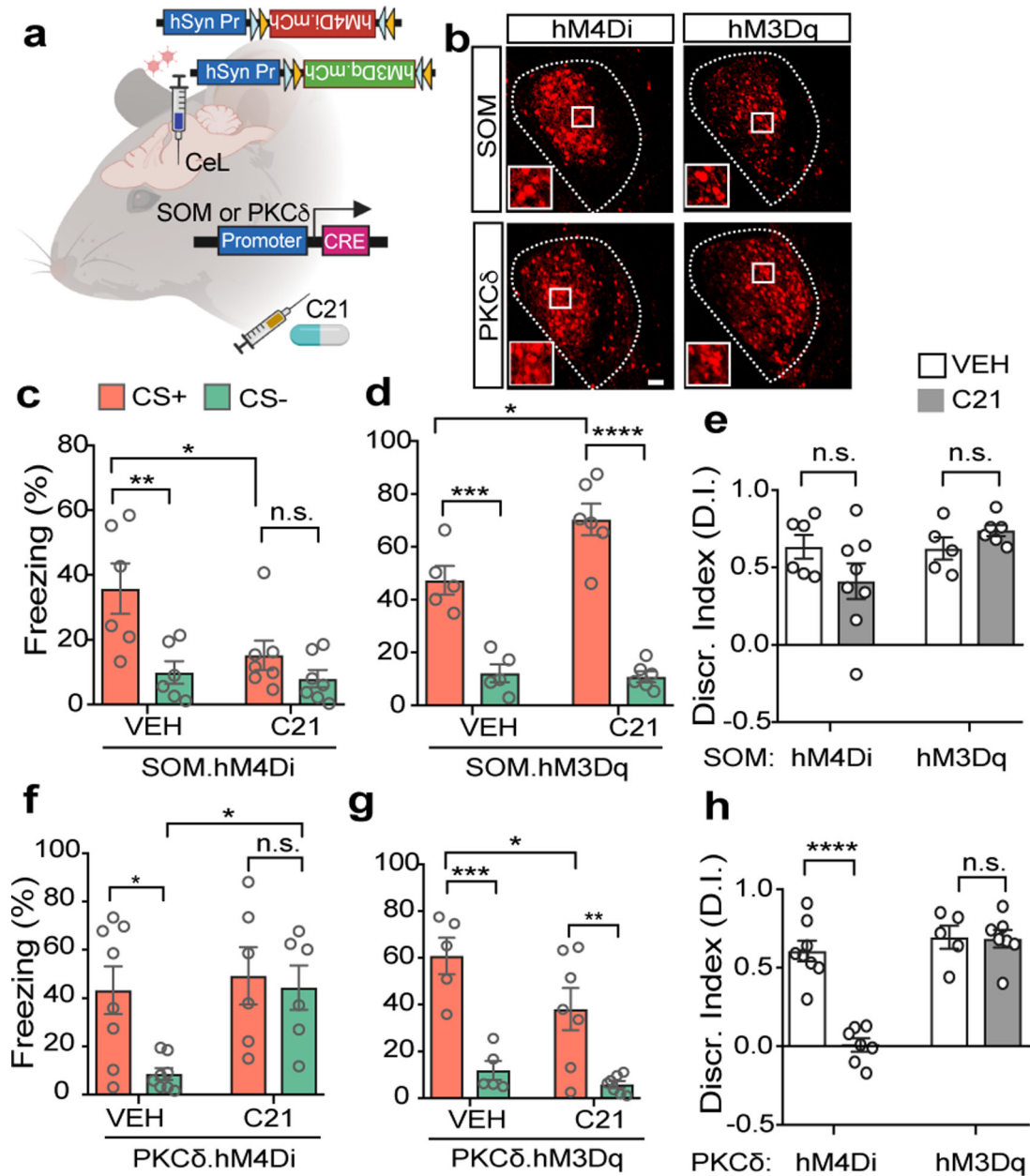


Figure 4. Conserved G-protein signaling pathways in CeL INs modulate threat and safety responses.

a) Chemogenetic strategy for expressing designer G_{ai} (hM4Di) or G_{aq} (hM3Dq) protein coupled DREADD receptors in CeL SOM and PKC δ INs.

b) Representative immunohistochemical images for mCherry fused to DREADD receptors in CeL SOM and PKC δ INs. Insets show higher magnification.

c) Conditioned-threat response to CS+ is significantly impaired for SOM.hM4Di +C21 group compared to VEH control. Effect of drug: $F(1,22)=5.39$, $p=0.0299$; effect of CS: $F(1,22)=11.76$, $p=0.0024$. $n[\text{VEH}]=6$ and $n[\text{C21}]=7$ animals.

d) Conditioned-threat response to CS+ is significantly increased in SOM.hM3Dq +C21 group compared with VEH control. Effect of drug: $F(1,18)=5.703$, $p=0.0281$. $n[\text{VEH}]=5$ and $n[\text{C21}]=6$ animals.

e) Discrimination-index for cued threat is normal across all SOM groups. Effect of genotype: $F(1,21)=3.015$, $p=0.097$, effect of drug: $F(1,21)=0.338$, $p=0.561$. SOM.hM4Di: $n[\text{VEH}]=6$ and $n[\text{C21}]=8$; SOM.hM3Dq: $n[\text{VEH}]=5$ and $n[\text{C21}]=6$ animals.

f) Conditioned safety response to CS- is significantly impaired in PKC δ .hM4Di animals administered with C21 compared to VEH control. Effect of drug: $F(1,24)=5.702$, $p=0.0252$; effect of CS: $F(1,24)=5.119$, $p=0.0330$. $n[\text{VEH}]=8$ and $n[\text{C21}]=6$ animals.

g) Conditioned-threat response to CS+ is significantly reduced in PKC δ .hM3Dq animals administered with C21 compared to VEH control. Effect of drug: $F(1,20)=4.77$, $p=0.041$; effect of CS: $F(1,20)=38.02$, $p<0.0001$. $n[\text{VEH}]=5$ and $n[\text{C21}]=7$ animals.

h) Discrimination-index for cued threat is significantly impaired for PKC δ .hM4Di mice +C21 mice compared to controls but unaltered for other groups. Effect of genotype: $F(1,23)=39.15$, $p<0.0001$; effect of drug: $F(1,23)=24.78$, $p<0.0001$. PKC δ .hM4Di: $n[\text{VEH}]=8$ and $n[\text{C21}]=7$; PKC δ .hM3Dq: $n[\text{VEH}]=5$ and $n[\text{C21}]=7$ animals.

Statistical tests: Two-way ANOVA with Bonferroni's post-hoc test (c-h). Data are presented as mean \pm SEM. * $p<0.05$, ** $p<0.01$, *** $p<0.001$, **** $p<0.0001$. n.s. nonsignificant. Scale bar, 50 μm .